SAND2018-11960PE

# Adventures in Vibrational Spectroscopy of Layered and Porous Materials

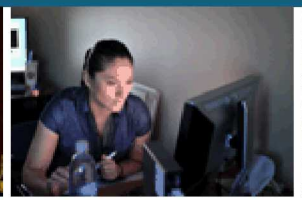

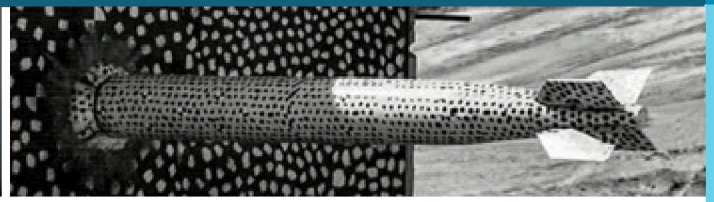

PRESENTED BY

Jacob A. Harvey

Sandia National Laboratories is a multimission laboratory managed and operated by National Technology & Engineering Solutions of Sandia, LLC, a wholly owned subsidiary of Honeywell International Inc., for the U.S. Department of Energy's National Nuclear Security Administration under contract DE-NA0003525.

# Acknowledgements


- **Sandia:**
  - Jeffery A. Greathouse
  - Dorina F. Sava Gallis
  - Charles J. Pearce
  - Mark K. Kinnan
- **Purdue University**
  - Cliff T. Johnston
- **Edgewood Chemical and Biological Center:**
  - Monica L. McEntee
  - Sergio J. Garibay
  - Erin M. Durke
  - Jared B. DeCoste

*This work was supported by the U.S. Department of Energy, Office of Science, Office of Basic Energy Sciences, Chemical Sciences, Geosciences, and Biosciences Division and Laboratory Directed Research and Development Program at Sandia National Laboratories. Sandia National Laboratories is a multimission laboratory managed and operated by National Technology and Engineering Solutions of Sandia, LLC., a wholly owned subsidiary of Honeywell International, Inc., for the U.S. Department of Energy's National Nuclear Security Administration under contract DE-NA-0003525.*

# Molecular Simulation of Phyllosilicates

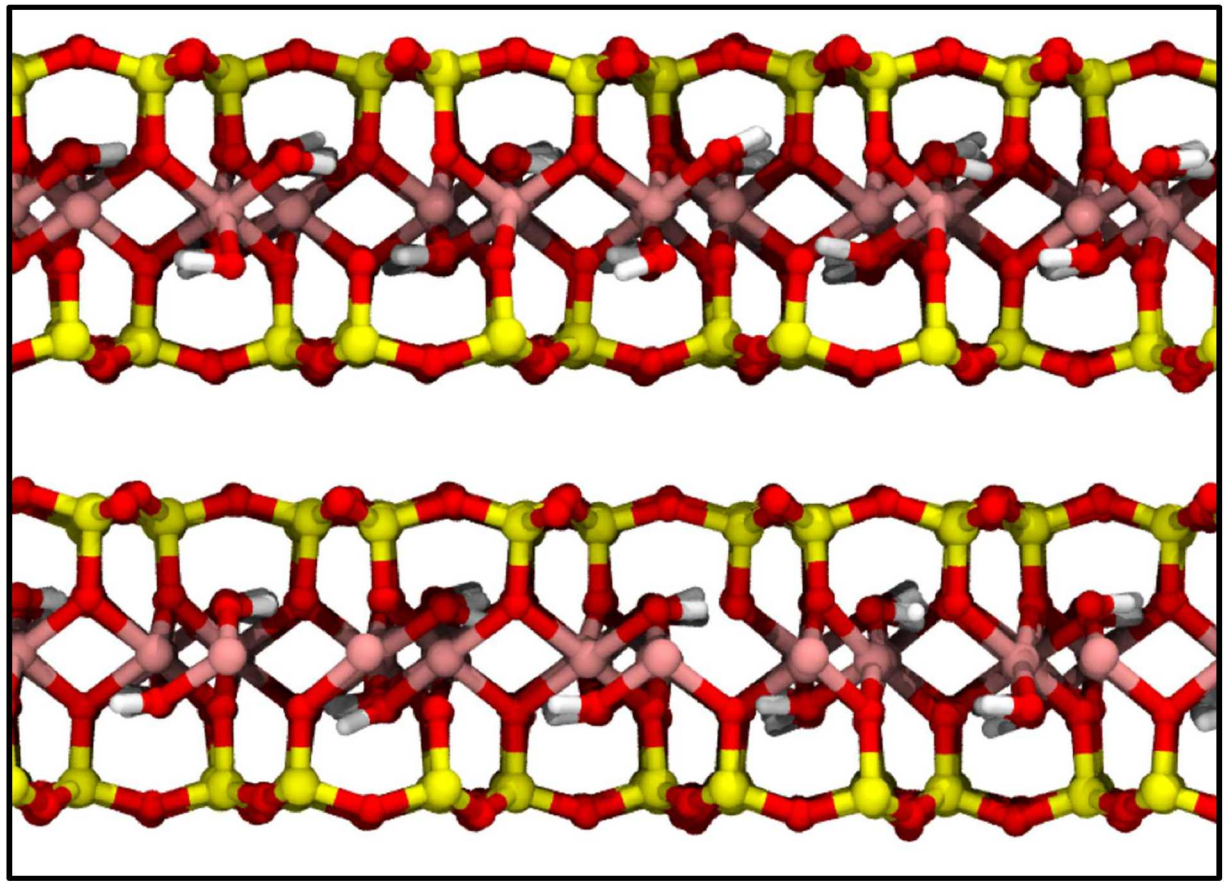

- Phyllosilicates exist as TOT stacked sheets
- Stacking disorder complicates structural analysis
- Complex chemistry with multicomponent systems, cation disorder, and vacancies
- Substitutions create a charge imbalance which is satisfied with cations in the interlamellar layer
- Swelling occurs which requires fully flexible force fields

# ClayFF Force Field Past Successes

## Swelling of Clays

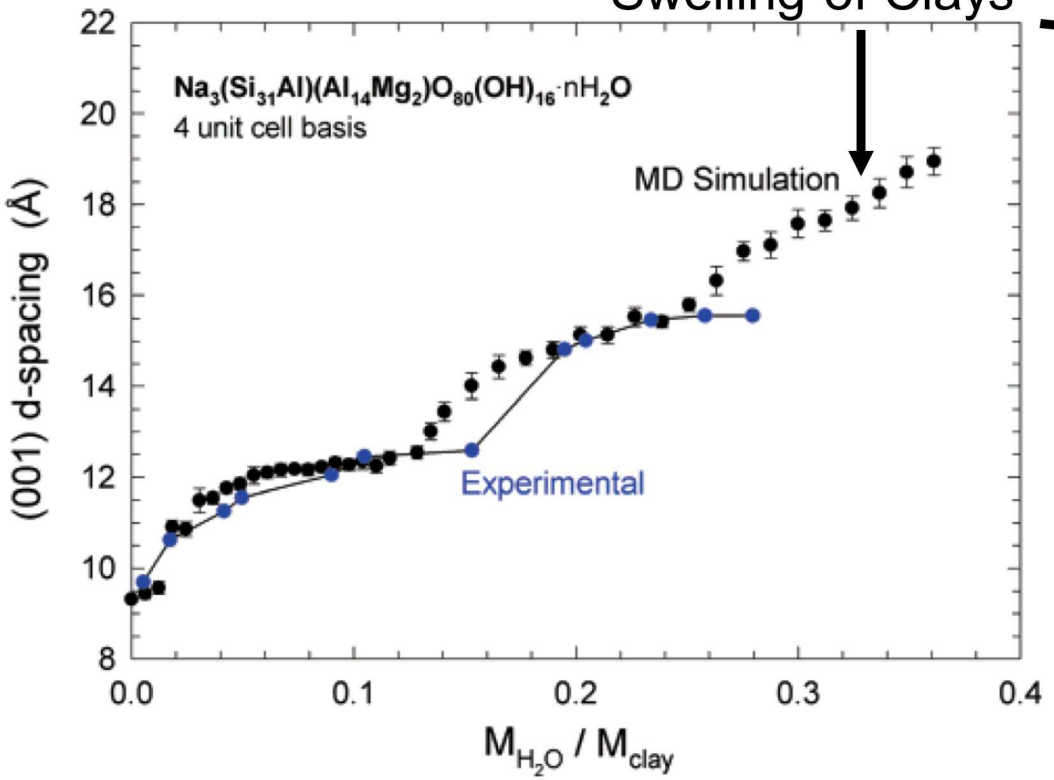


$$E_{total} = E_{Coul} + E_{VDW} + E_{BondO-H}$$

$$E_{total} = \frac{q_i q_j}{4\pi\epsilon_\circ r} + 4\epsilon_{ij}\left[\left(\frac{\sigma_{ij}}{r}\right)^{12} - \left(\frac{\sigma_{ij}}{r}\right)^{6}\right] + D_\circ\left[1 - e^{-\alpha(r-r_\circ)}\right]^2$$

| | | 0W | | 1W | | 2W | |
|---|---|---|---|---|---|---|---|
| | | this work | exp | this work | exp | this work | exp |
| $Na^+$ | mont | 9.35 | 9.6–9.8[21,58–61] | 12.17 | 12.3–12.6[21,55,58] | 14.91 | 14.9–15.6[21,55,58,59,61] |
| | beid | 9.42 | 9.6–9.8[a,b,c] | 12.26 | 12.4–12.5[a,b,c], | | 15.2–15.4[a] |
| $Cs^+$ | mont | 10.53 | 10.7–11.2[21,58–61] | 12.28 | 11.9–12.6[58–60] | | |
| | beid | 10.93 | | 12.27 | | | |
| $Ca^{2+}$ | mont | 9.35 | | 11.95 | | 14.61 | 15.4–16.0[21,62,63] |
| | beid | 9.32 | | 11.94 | 11.78[d] | | 15.50[b] |
| $Mg^{2+}$ | mont | 9.30 | | | | 13.61 | 13.9–14.9[64,65] |
| | beid | 9.30 | | 12.17 | | 13.51 | |

## Binding of organics at clay surfaces

| | | binding energy (kcal·mol$^{-1}$) | |
|---|---|---|---|
| surface | complex | DFT | classical |
| gas phase | $Ca^{2+}$–$DHNA^-$ | −345.4 | −365.7 |
| | $Na^+$–$DHNA^-$ | −164.5 | −150.1 |
| | $Na^+$–toluene | −36.1 | −13.1 |
| pyrophyllite | $Na^+$ | −101.5 | −69.1 |
| | $Ca^{2+}$ | −350.1 | −238.2 |
| | DHNA | −16.3 | −9.7 |
| | $Ca^{2+}$–$DHNA^-$ | −465.6 | −402.8 |
| kaolinite | $Na^+$ | −89.4 | −74.2 |
| | DHNA | 11.6 | −12.4 |
| | $Na^+$–$DHNA^-$ | −188.8 | −200.8 |
| | toluene | −13.2 | −13.4 |
| | $Na^+$–toluene | −126.7 | −91.0 |
| | hexane | −11.2 | −8.6 |
| | cyclohexane | −10.7 | −7.6 |

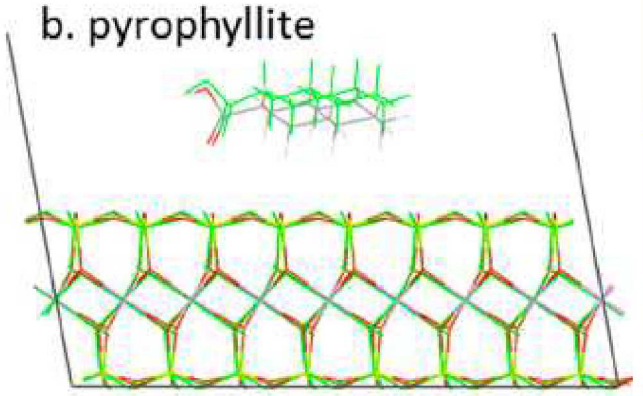


- Clayff has successfully modeled interactions, structures, and dynamics in bulk clays at the basal surface
- **But what about clay edges?**

Cygan, R.T. et al.; *J. Phys. Chem. B* **2004**, 108, 1255-1266
Teich-McGoldrick, S.L. et. al; *J. Phys. Chem. C* **2015**, 119, 20880
Greathouse, J.A. et. al; *J. Phys. Chem. C* **2017**, 121, 2273-22786

# Effect of Angle Bending Parameters on Clay Structure

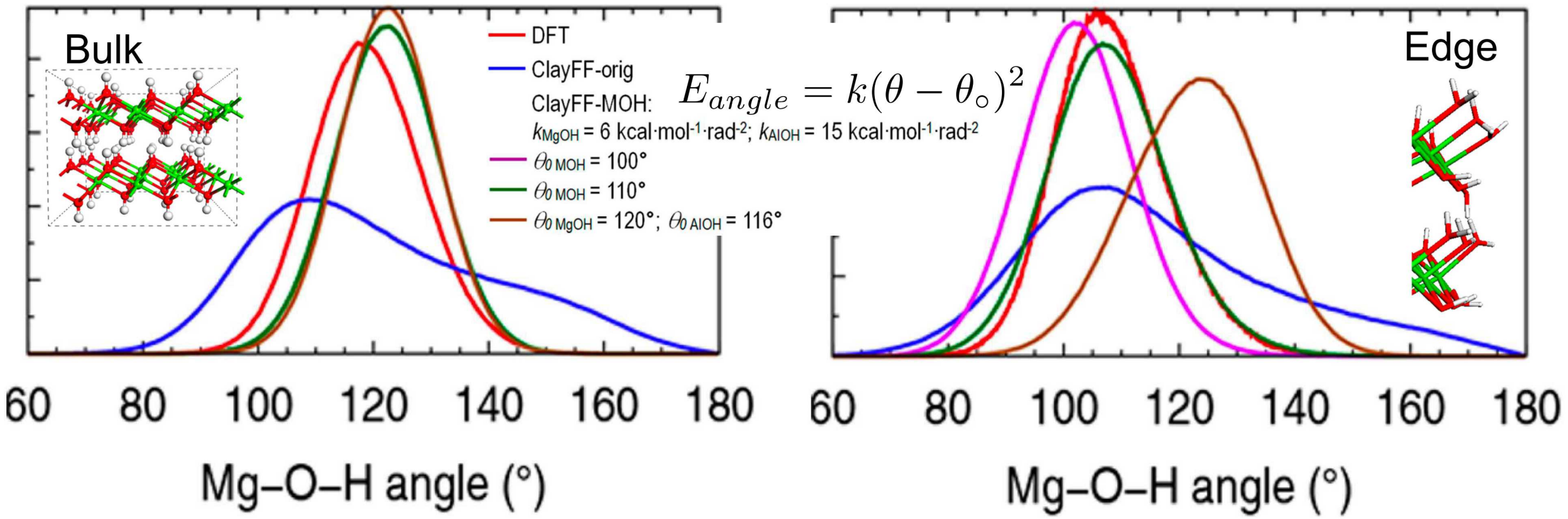


- Angle distributions from classical simulations with an angle bending term more closely match results from DFT simulations

Pouvreau, M. et. al; *J. Phys. Chem. C* **2017**, 121, 14757-14771

# Effect of Angle Bending Parameters on Clay Structure

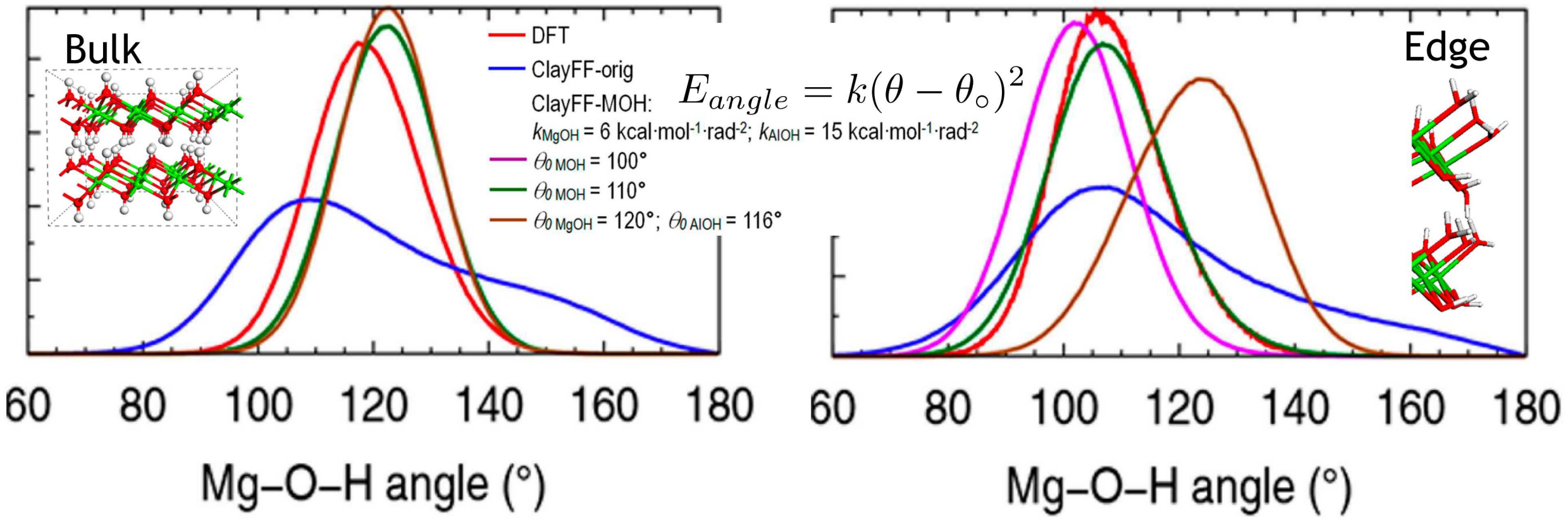


- Angle distributions from classical simulations with an angle bending term more closely match results from DFT simulations
- **Is this improved structure observable via infrared spectroscopy?**

Pouvreau, M. et. al; *J. Phys. Chem. C* **2017**, 121, 14757-14771

# Pyrophyllite Model for Density Functional Theory Calculations

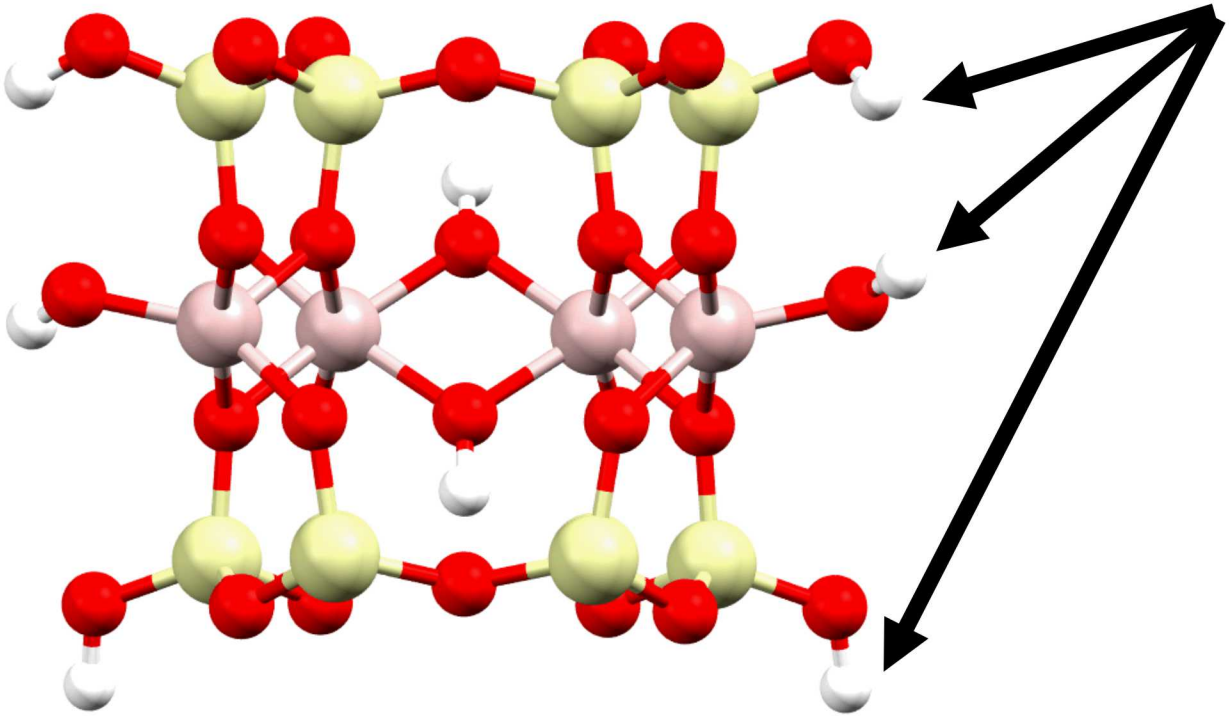

OD spectra replaces edge H's with D's

- Vibrational spectrum calculated on periodic structures using DFPT

$$I(\omega) = \sum_{\alpha=1}^{3} \left| \sum_{s=1}^{M} \sum_{\beta=1}^{3} Z^{*}_{\alpha\beta}(s) e_{\beta}(s) \right|^{2}$$

Cartesian polarizations

Vibrational eigenvector

Born effective charge of $s^{th}$ atom

- 1x1x1 unit cell, (010) and (110) faces of pyrophyllite, 1 edge cut on each face
- VASP optimized/vibrational frequencies (PAW method, PBESol functional, DFT-D3 VDW corrections)
- Deuterate edges to compare to ATR-FTIR experiments where deuteration will only occur at edges
- Deuterated spectra are calculated from the protonated optimized structure

*Phys. Rev. B* **1991**, 43, 7231-7242; *J. Chem. Phys.* **1994**, 100, 8537-8539
*Rev. Mod. Phys.* **2001**, 73, 515-562; *J. Phys. Condens. Matt.* **2010**, 22, 265006

# VASP Calculated IR Spectra of Protonated Pyrophyllite Edges

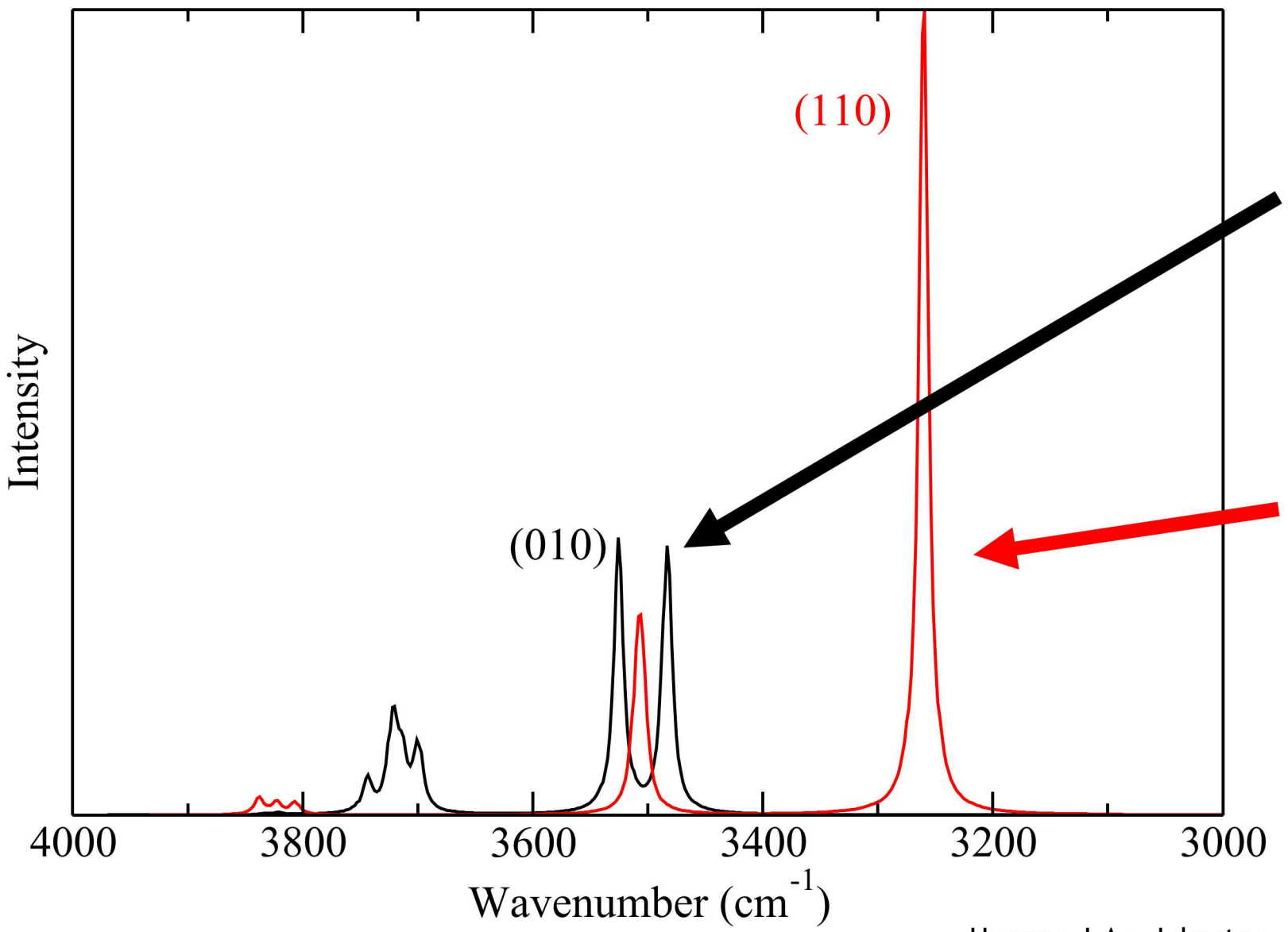


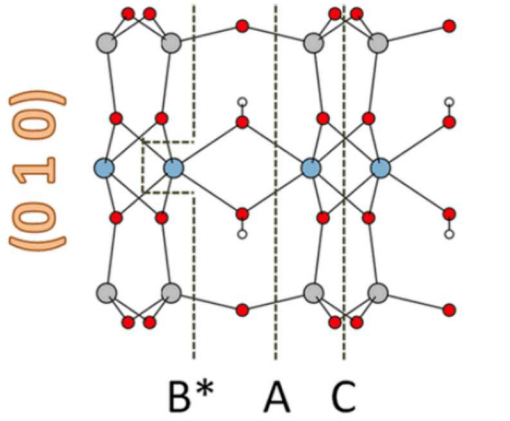


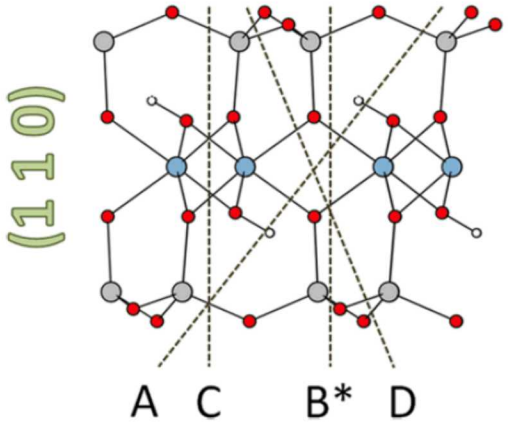


Harvey, J.A.; Johnston, C.T.; Greathouse, J.A.; *Chem. Comm.*, submitted

# Hydrogen Bonding Features Observed in IR Spectra

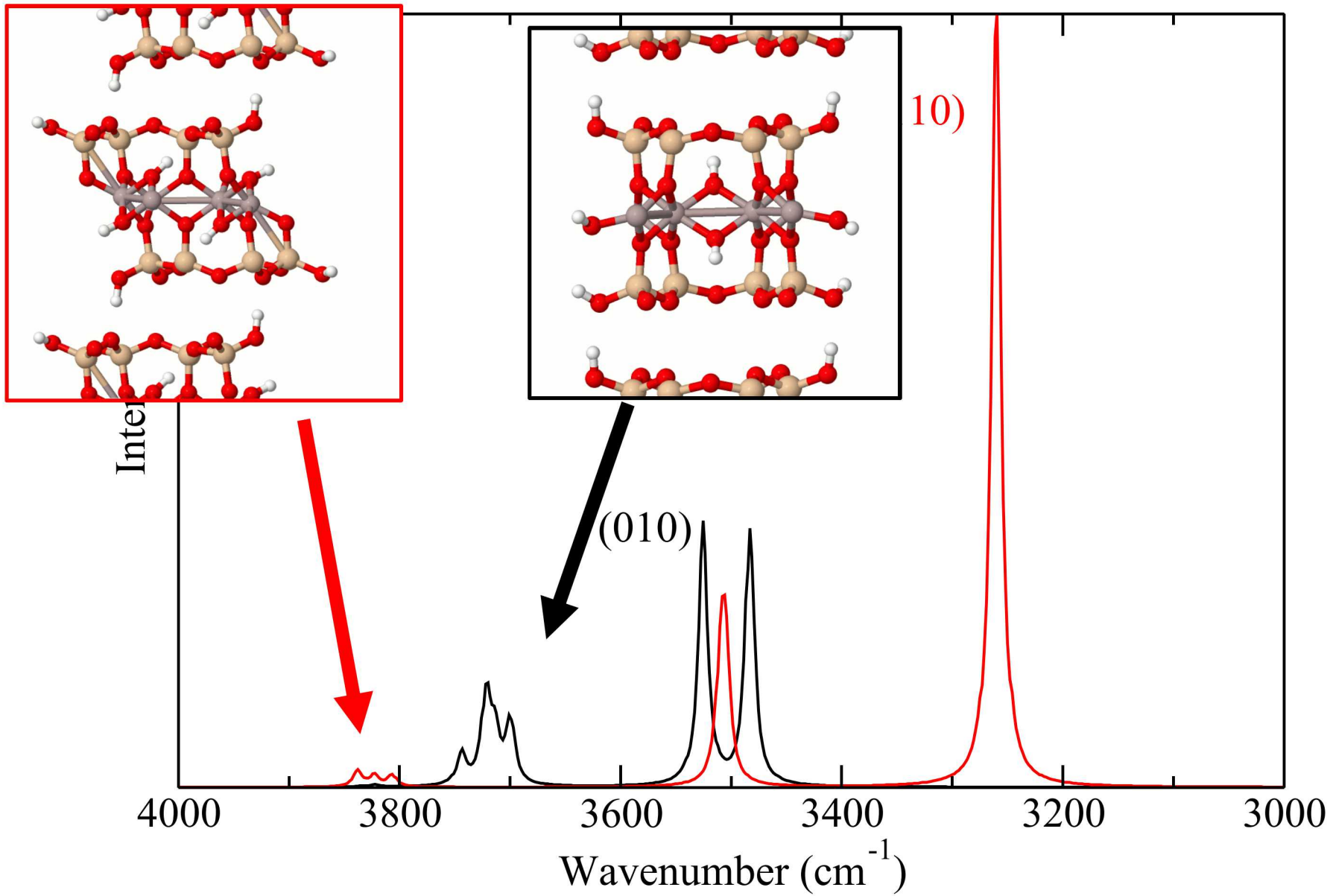


Harvey, J.A.; Johnston, C.T.; Greathouse, J.A.; *Chem. Comm.*, submitted

# Hydrogen Bonding Features Observed in IR Spectra

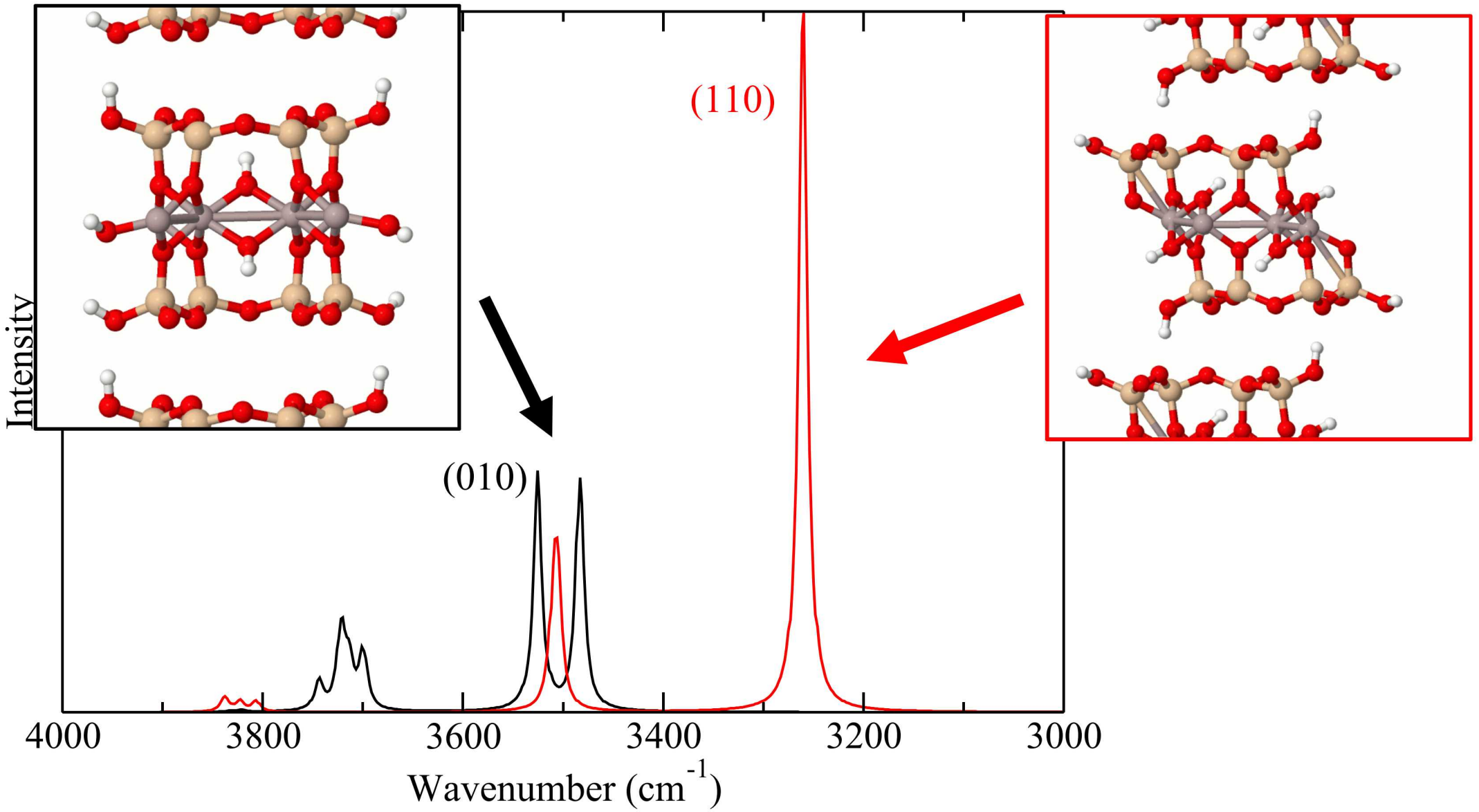


Harvey, J.A.; Johnston, C.T.; Greathouse, J.A.; *Chem. Comm.*, submitted

# The Effect of Deuteration on IR Spectrum

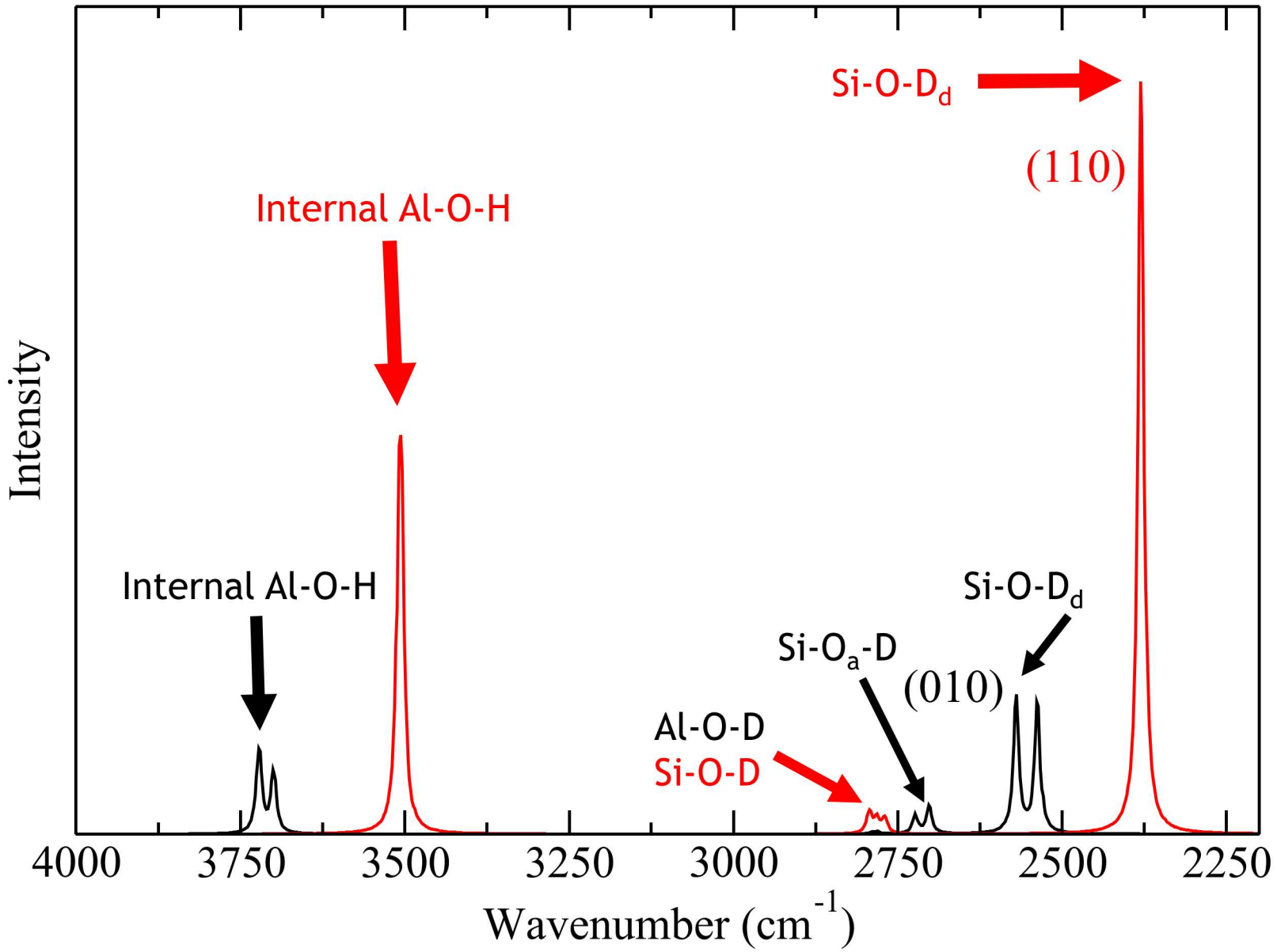


Harvey, J.A.; Johnston, C.T.; Greathouse, J.A.; *Chem. Comm.*, submitted

# Molecular Dynamics Simulations of Pyrophyllite

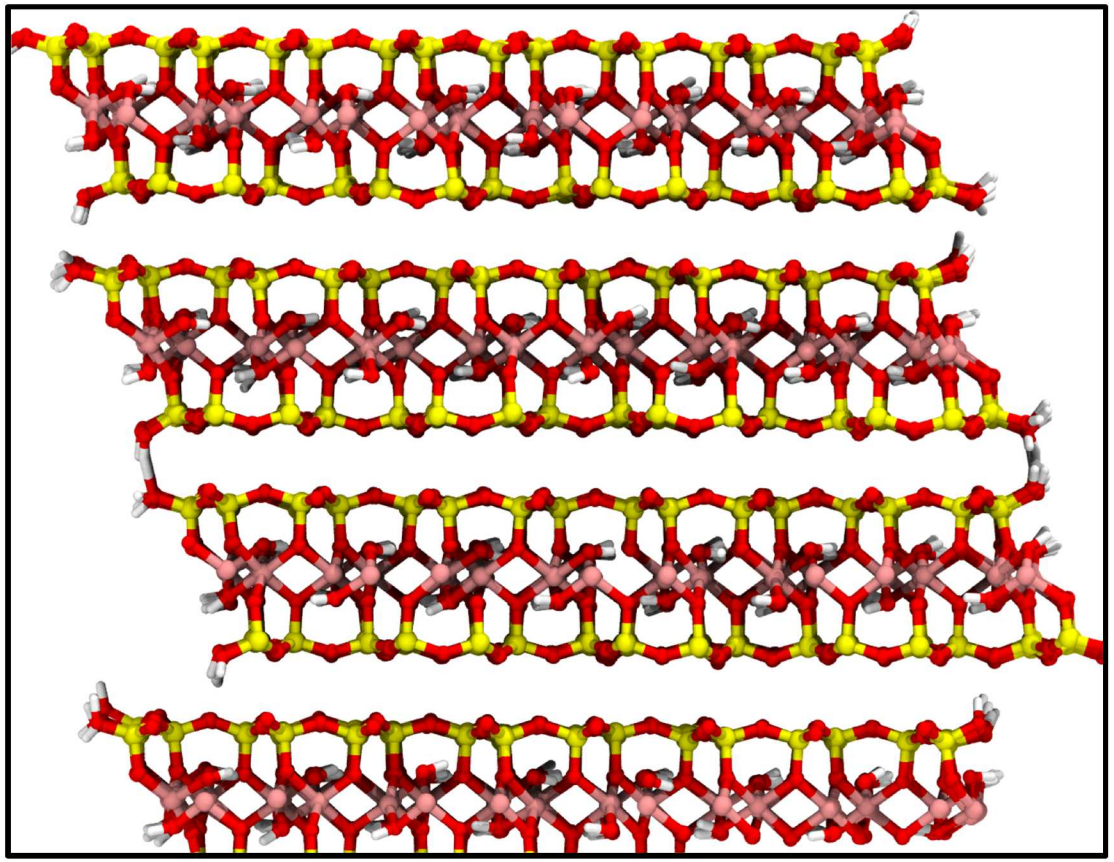

- 6x4x4 box created from optimized unit cells (3984 atoms)
- ClayFF force field with Al-O-H and Si-O-H angle bending parameters:

$$E_{angle} = k(\theta - \theta_\circ)^2$$

$$k = 15\ kcal/mol$$

$$\theta_\circ Si - O - H = 100^\circ$$

$$\theta_\circ Al - O - H = 110^\circ$$

- H/D atoms have different masses but same force field parameters
- NVT ensemble controlled by Nose-Hoover thermostat
- 10 ns equilibration time
- 5 ns of production run time, vibrational analysis over 1 ns
- Infrared Spectrum:

$$I(\omega) = \frac{1}{2\pi}\int_{-\infty}^{\infty} dt e^{-i\omega t}\langle \vec{M}(t)\cdot\vec{M}(0)\rangle \longrightarrow I(\omega) = \frac{1}{2\pi\omega^2}\int_{-\infty}^{\infty} dt e^{-i\omega t}\langle \frac{d\vec{M}(t)}{dt}\cdot\frac{d\vec{M}(0)}{dt}\rangle$$

$$\vec{M}(t) = \sum_i^{n_{atoms}} q_i\vec{r}_i(t) \qquad \frac{d\vec{M}(t)}{dt} = \sum_i^{n_{atoms}} q_i\vec{v}_i(t)$$

Al-O-H: Pouvreau, M. et. al; *J. Phys. Chem. C* **2017**, 121, 14757-14771
Si-O-H: Pouvreau, M. et. al **2017,** *in prep*.

# IR Spectrum of Bulk Pyrophyllite; Inclusion of Angle Bending Term

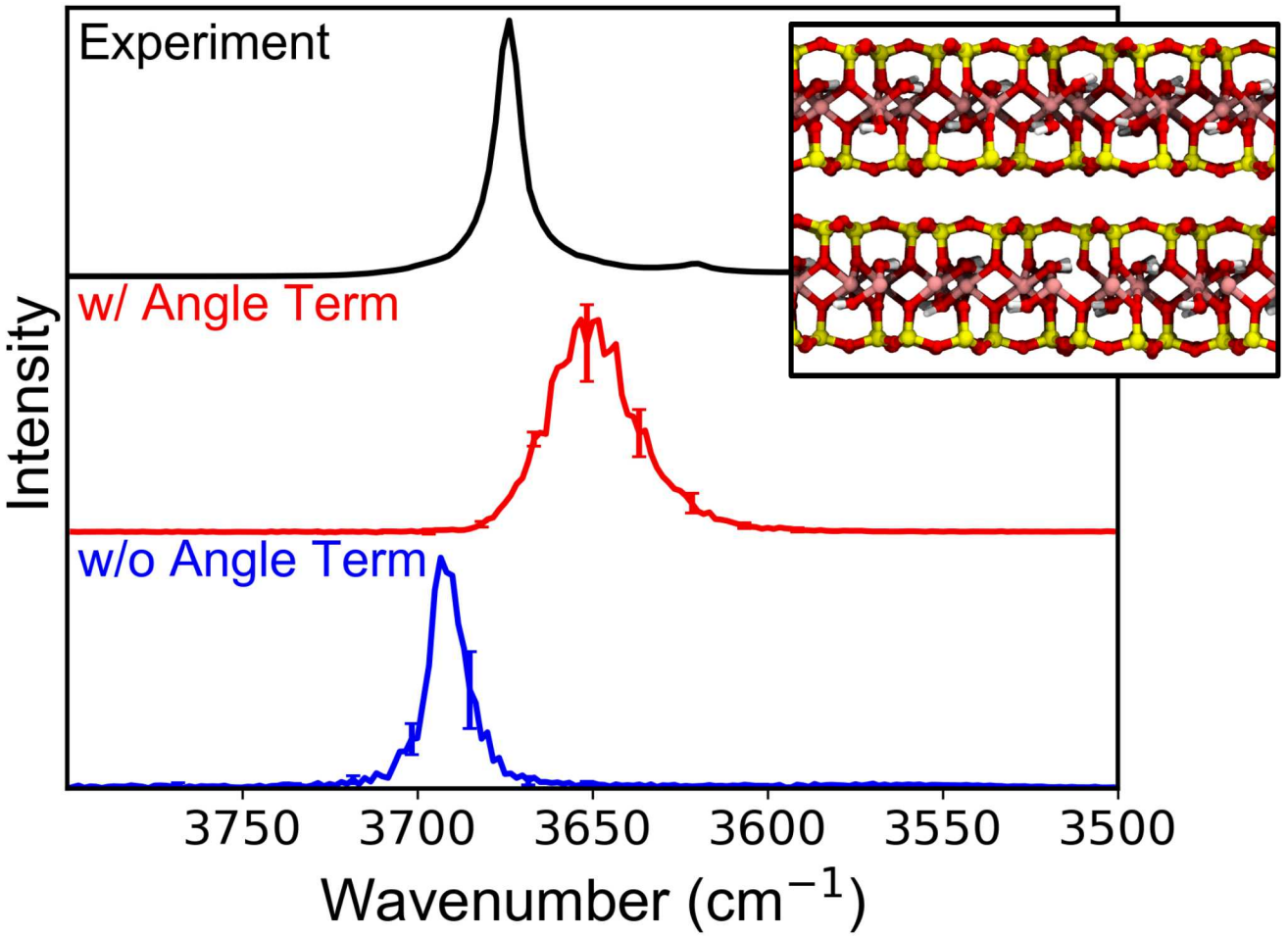


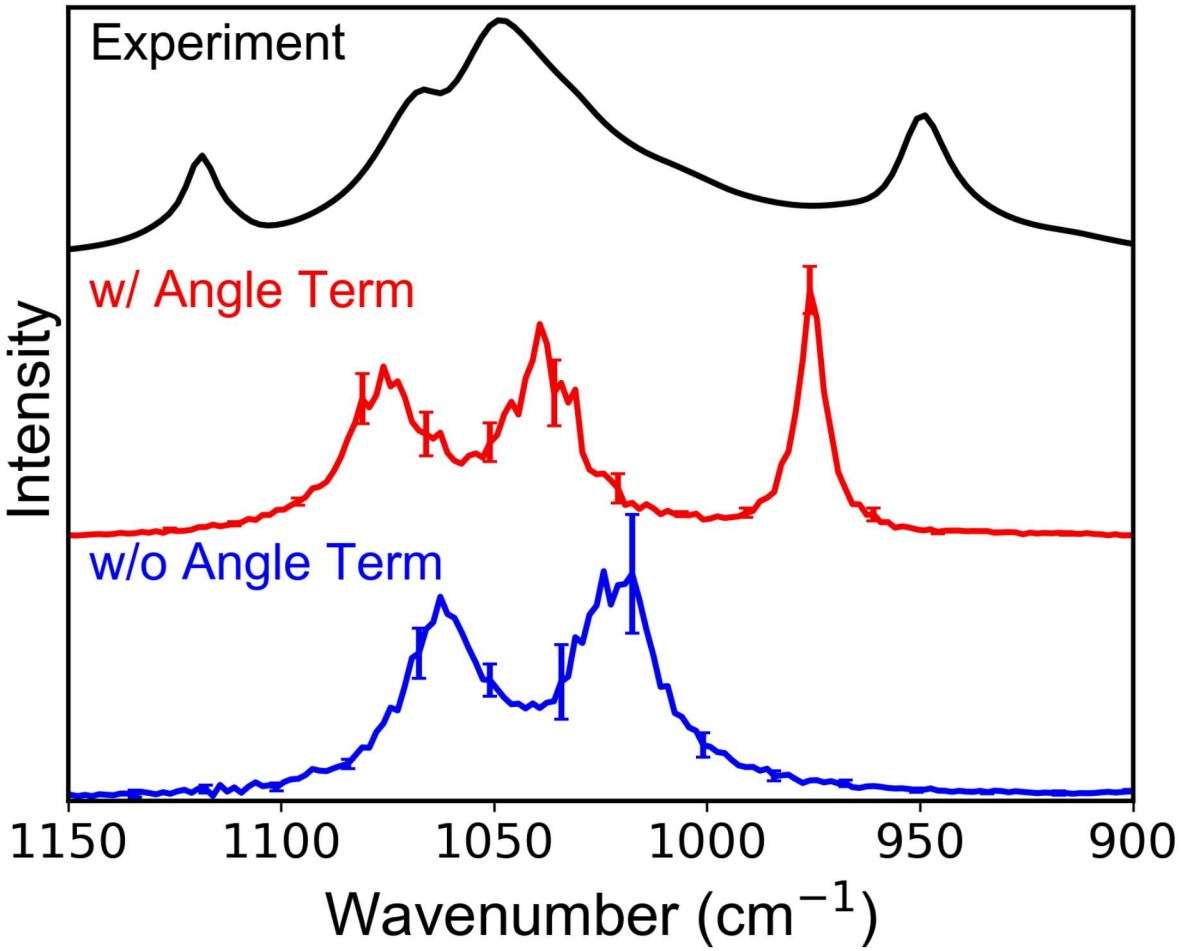


Harvey, J.A.; Johnston, C.T.; Greathouse, J.A.; *Chem. Comm.*, submitted

# IR Spectrum of (110) Pyrophyllite Edge

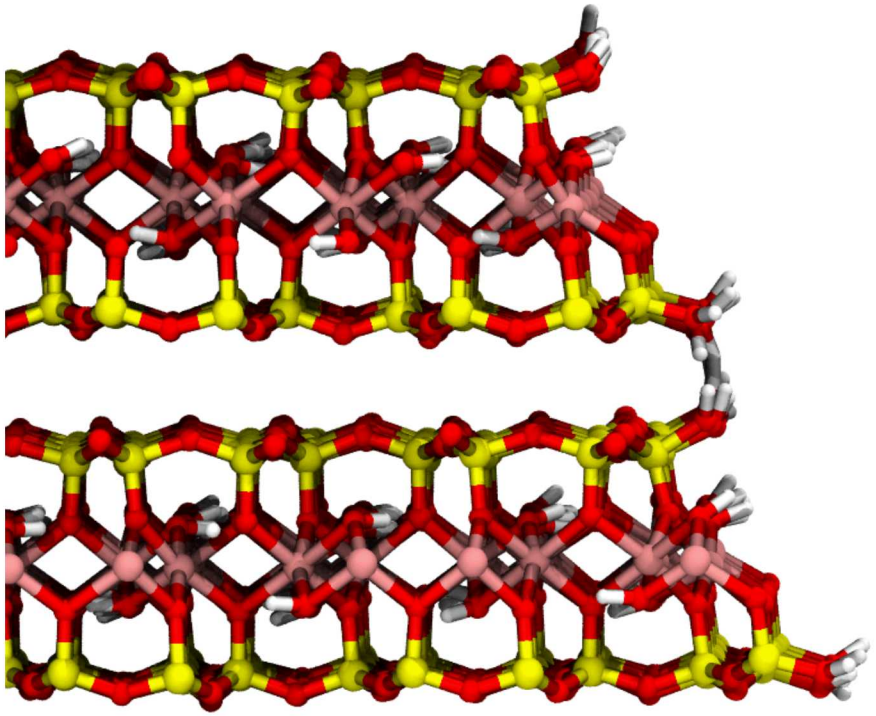

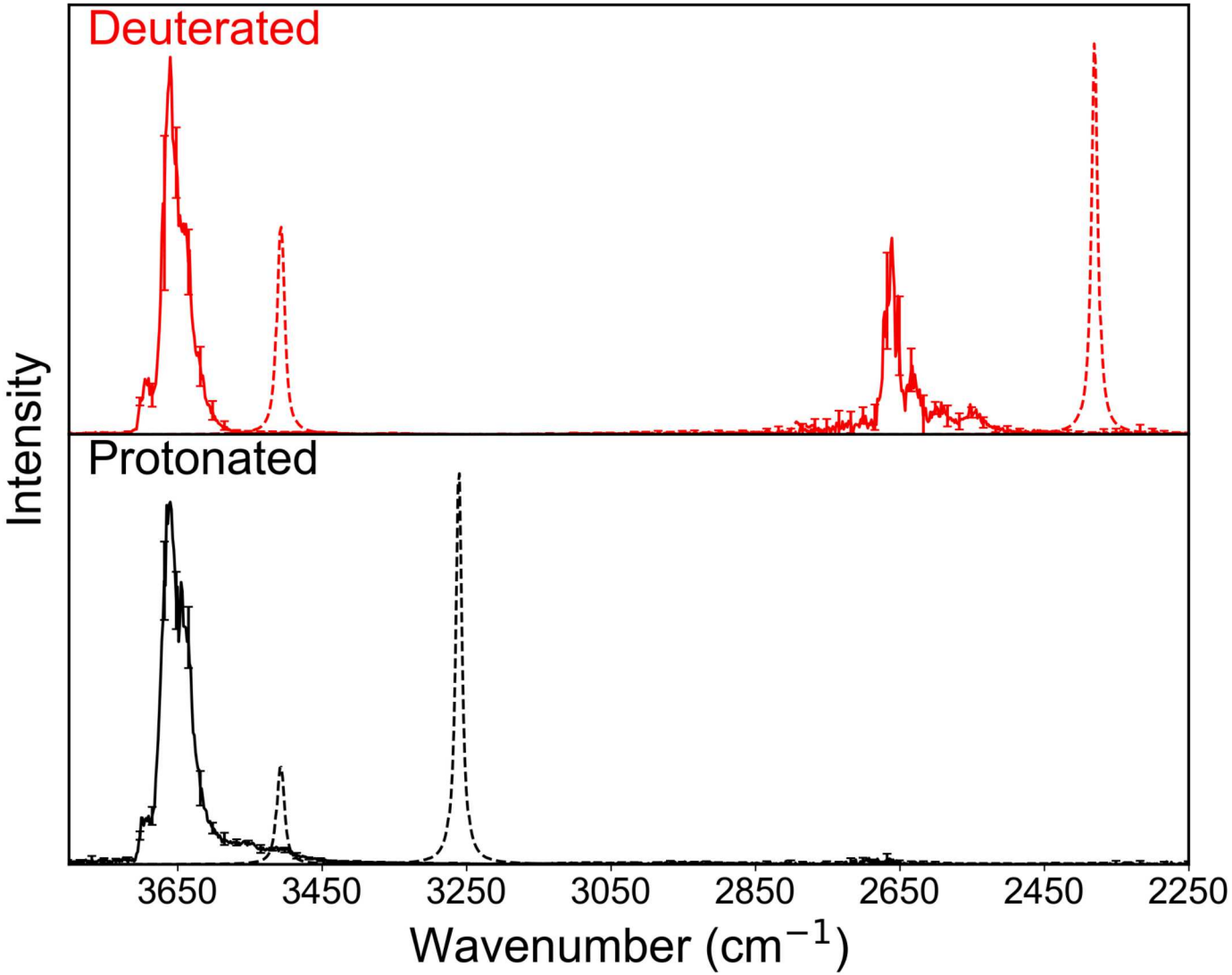


Harvey, J.A.; Johnston, C.T.; Greathouse, J.A.; *Chem. Comm.*, submitted

# Direct Comparison of Simulated Pyrophyllite Spectrum to Experiments

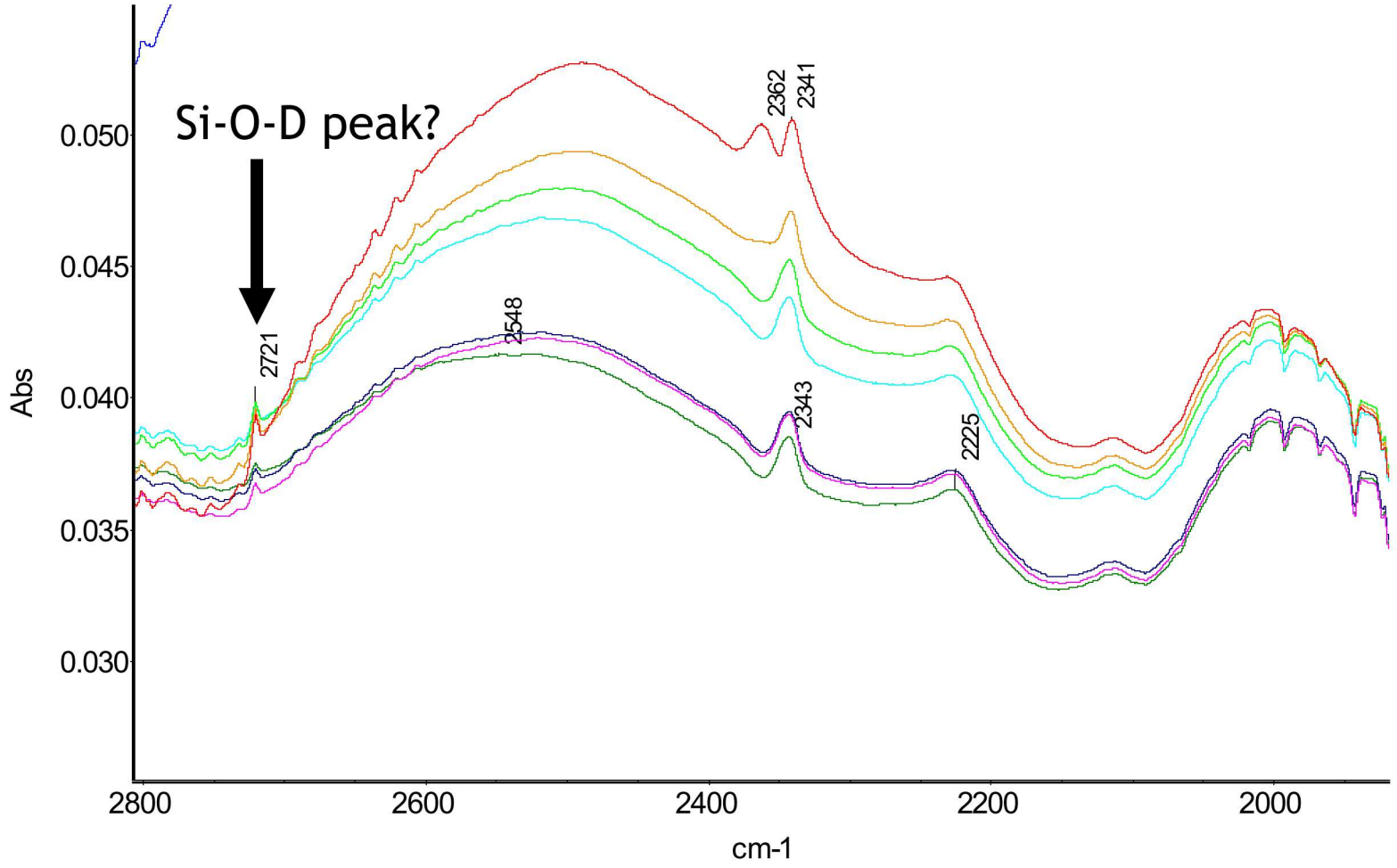


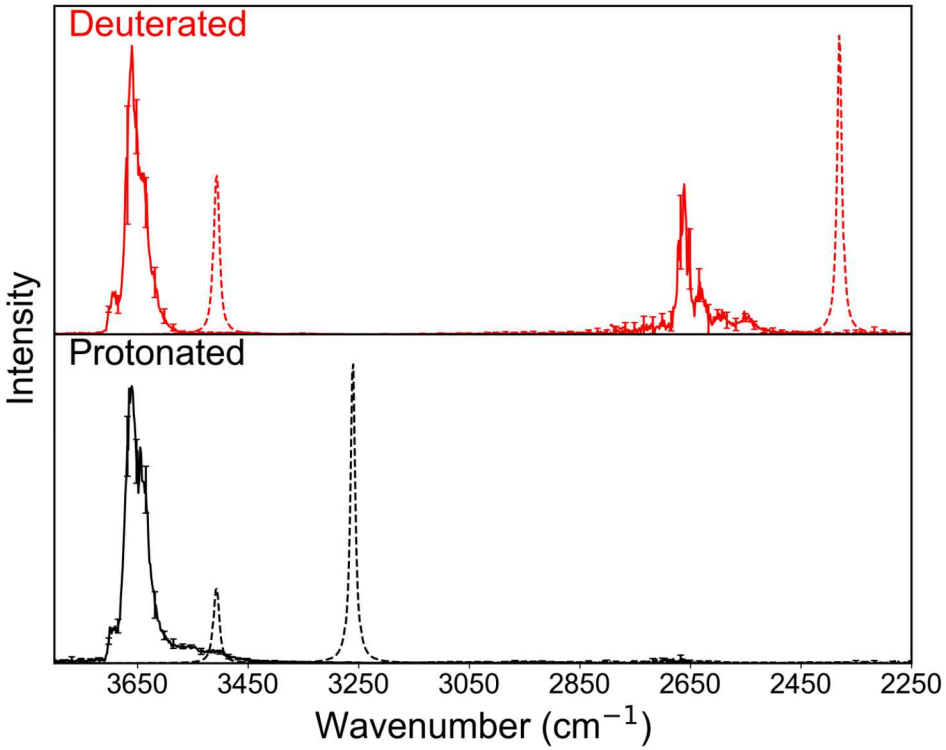


Harvey, J.A.; Johnston, C.T.; Greathouse, J.A.; *Chem. Comm.*, submitted

# Conclusions

ClayFF angle bending terms improve simulated clay edge structure

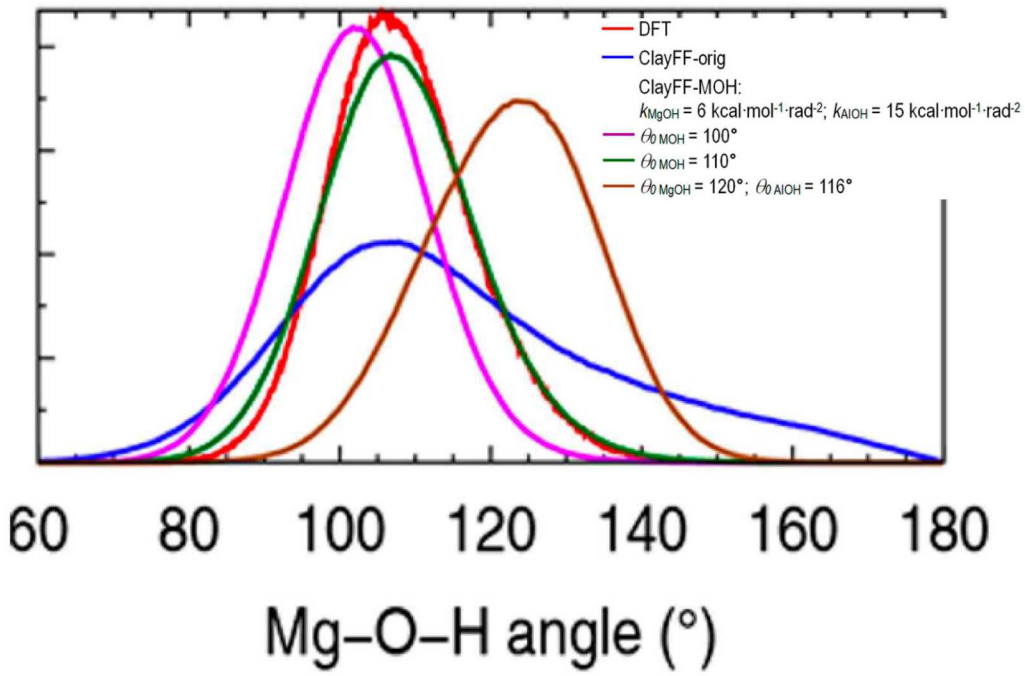


Improved clay structure leads to improved agreement in clay IR spectrum

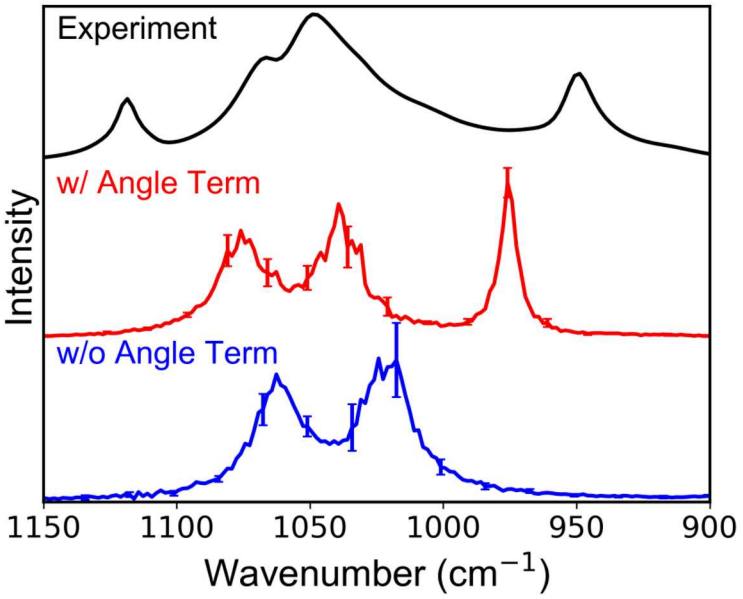


Direct observation of clay edge via IR spectroscopy

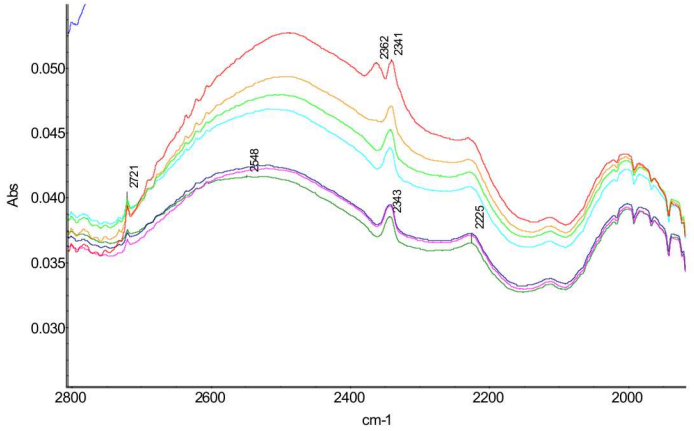


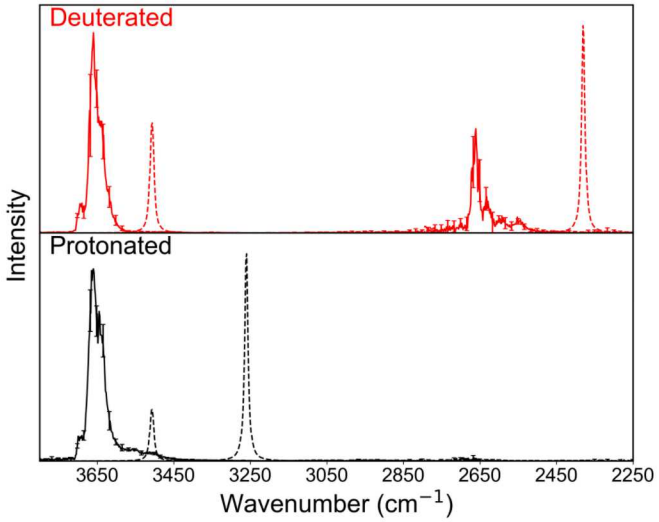

# Goal: Investigate chemistries to degrade organophosphorous compounds in water free environments; identify suitable simulants

**Billion-fold Acceleration of the Methanolysis of Paraoxon Promoted by $La^{3+}$ complexes**

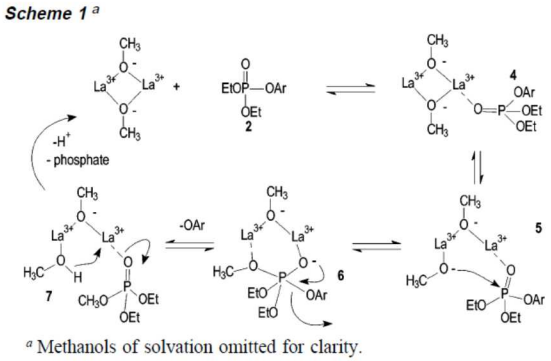


**La $^{3+}$ catechol-functionalized POPs show accelerated activity towards methanolysis**

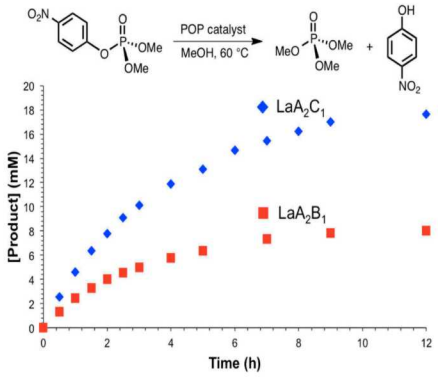


**Methanolysis of organophosphates is accelerated by La-based catalysts**

- The molecular structure/reactivity of simulants vs. Chemical Warfare Agents (CWAs) is different
- Tests performed on CWAs are not trivial and conducted only at authorized facilities
- Simulants allow screening of materials

Increase in Correlation to Live Agent?

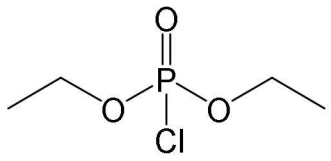

**Diethyl Chlorophosphate (DECP)**

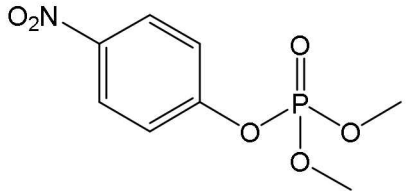

**Dimethyl Nitrophenylphosphate (DMNP)**

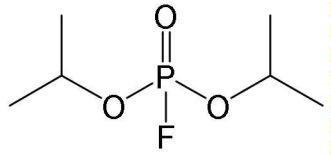

**Diisopropyl Fluorophosphate (DFP)**

*J. Am. Chem. Soc.* **2003**, *125*, 7602-7607.
*ACS Catal.* **2013**, *3*, 1454−1459

# Rare-Earthed Based MOFs: 3D Structure

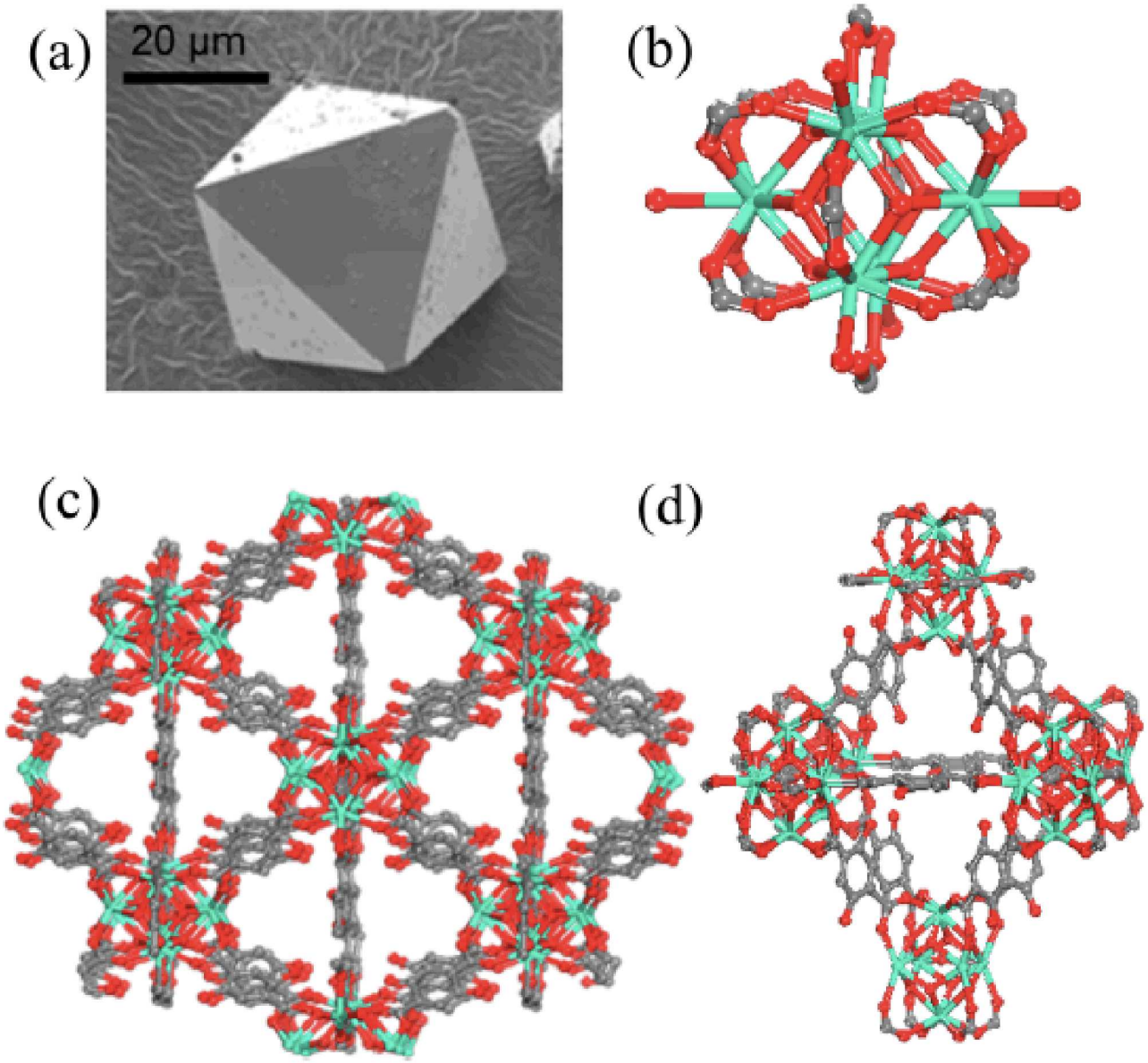


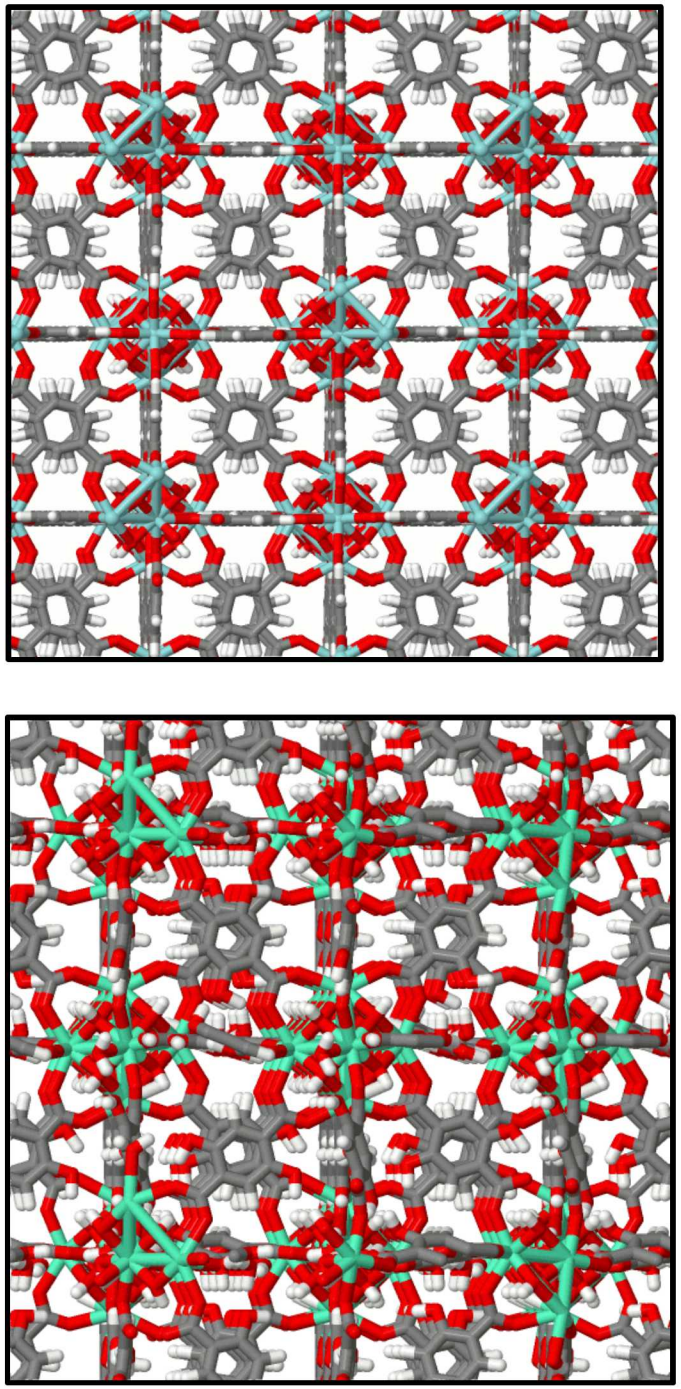

*ACS Appl. Mater. Interfaces* **2017**, 9, 22268-22277

# Importance of Adsorption of Organophosphorous Compounds in MOFs

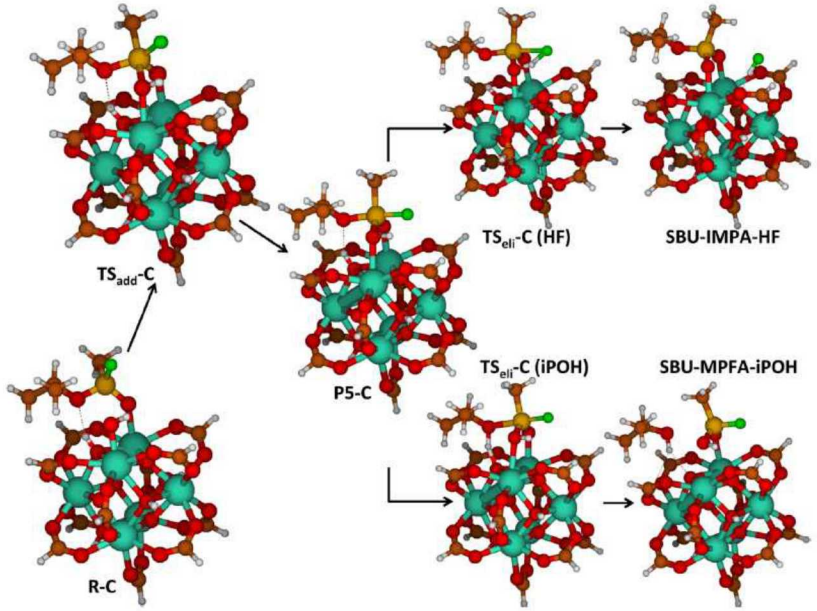


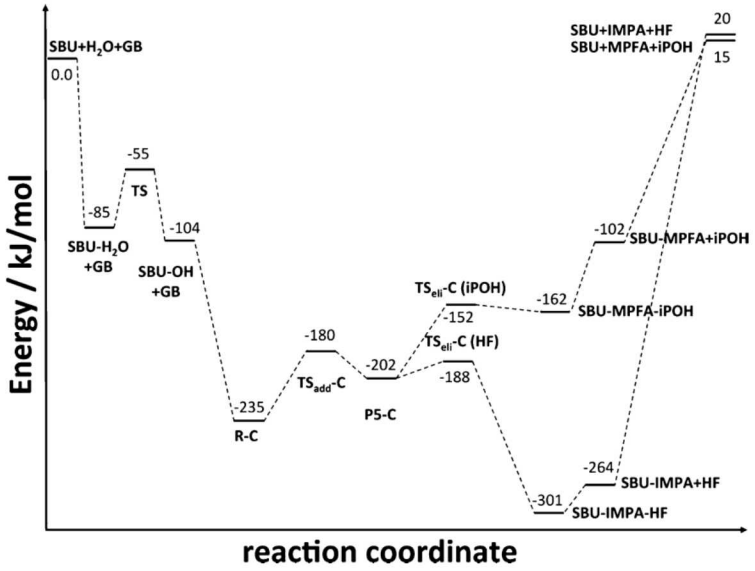


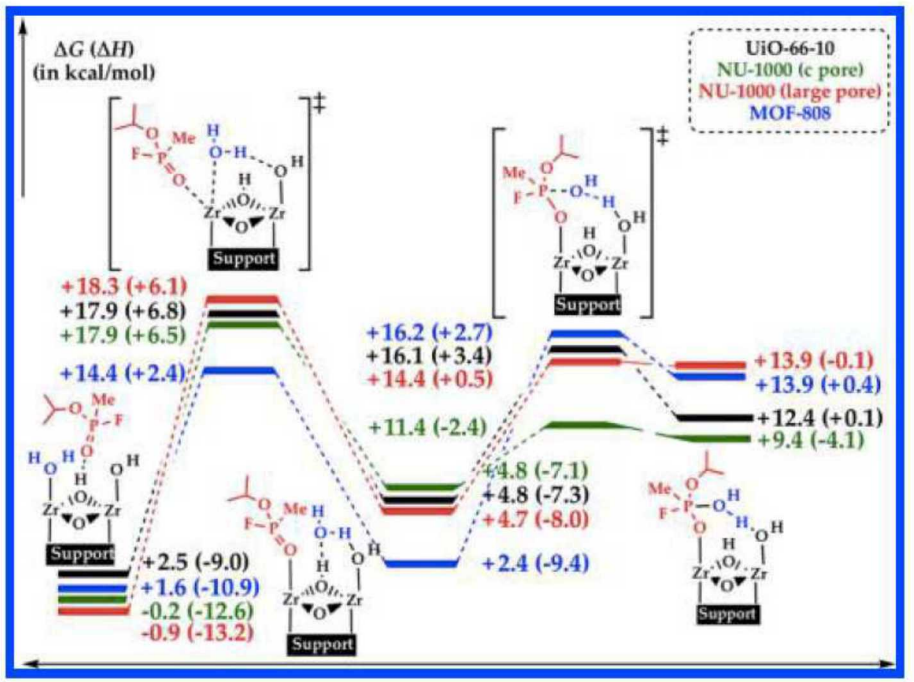


- Adsorption of GB in MOFs is a critical first step towards the degradation, however this process is poorly understood
- Assumption that degradation happens via adsorption onto a defect site has never been confirmed experimentally.

Troya, D., *J. Phys. Chem. C*, **2016**, 120, 29312-29323
Momeni, M. R.; Cramer, C. J., *ACS Appl. Mater. Interfaces*, **2018**, 10, 18435-19439

# Missing Linker and Structural Defect Metal Sites

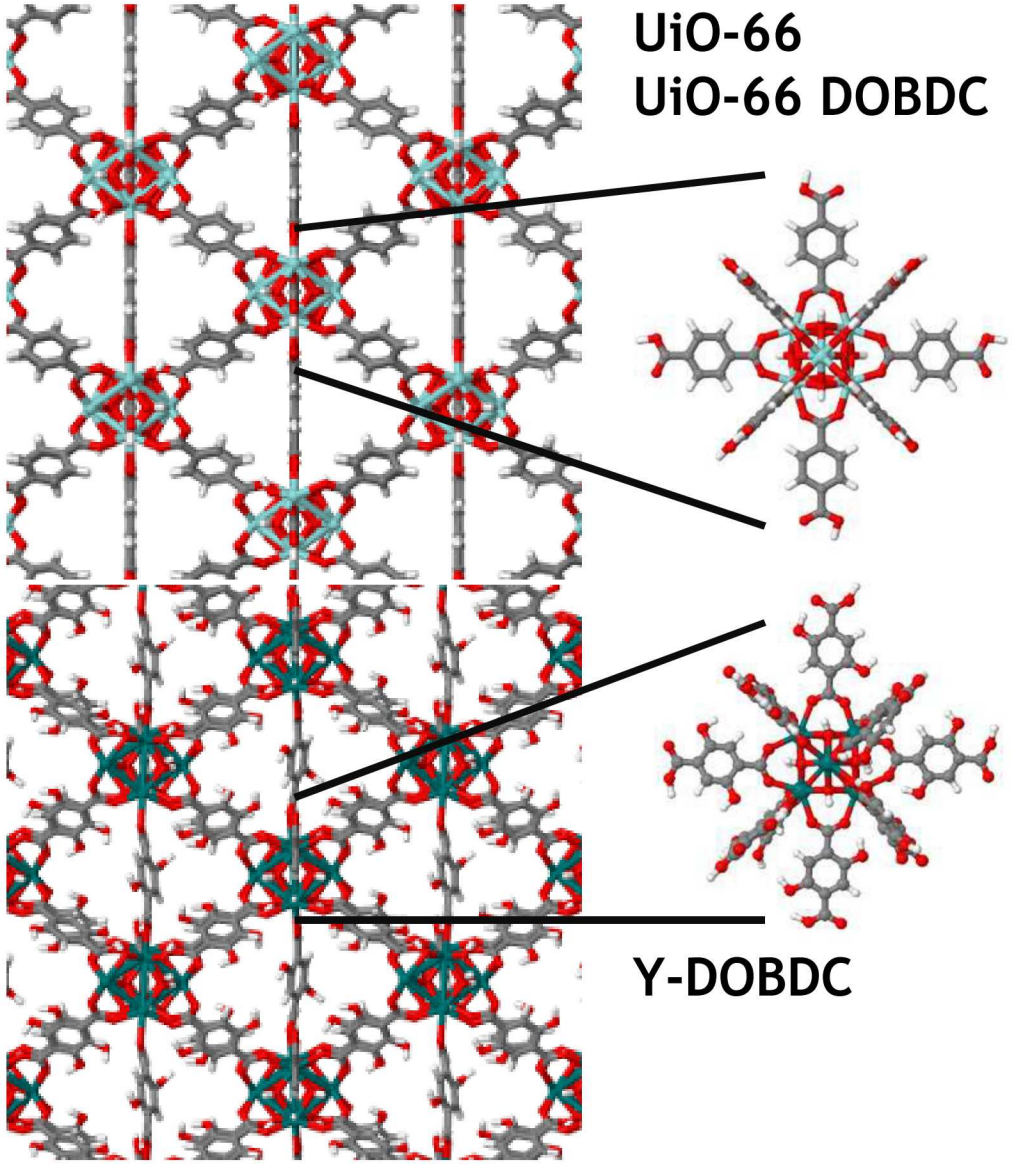

**UiO-66**
**UiO-66 DOBDC**

**Y-DOBDC**



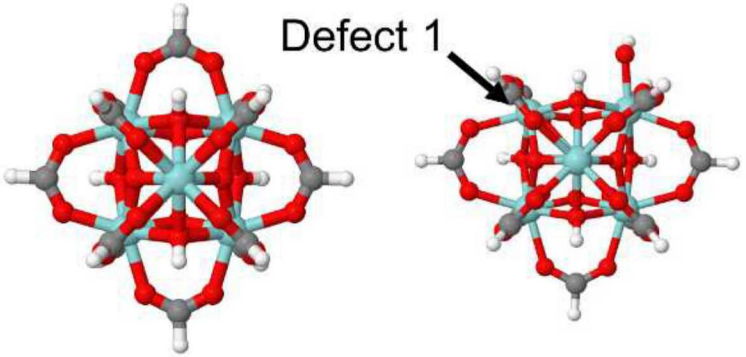




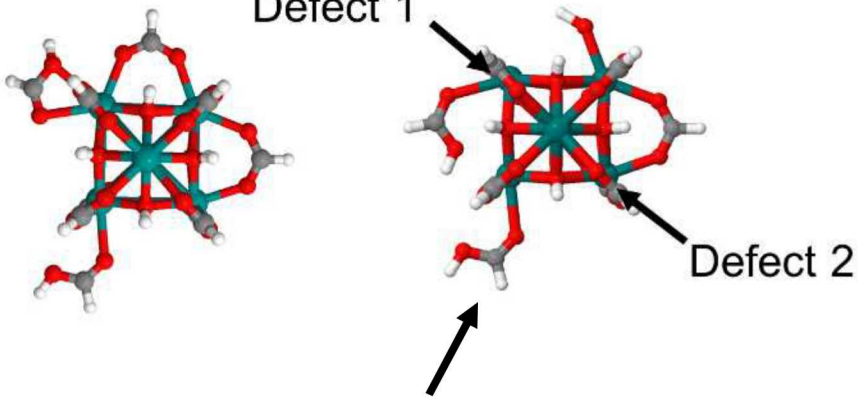


DECP

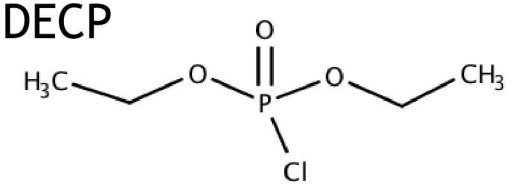


DFP

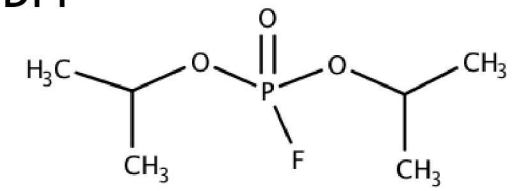


GB

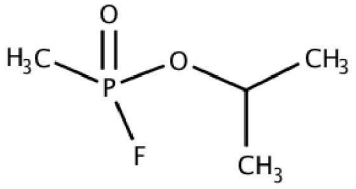


2 unique defects possible in Y-DOBDC:

- Missing linker defect identical to UiO-66 (defect 1)
- Twisted linker defect (defect 2)

# Computational Methods

Cluster Models:

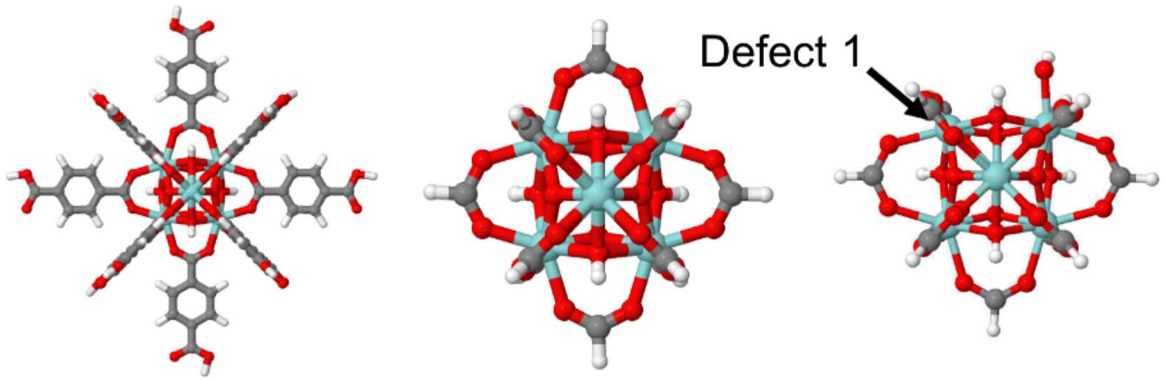


- Representative clusters cut from periodic structures
- Each cluster consists of full hexanuclear metal cluster and 12 linkers
- Linkers shortened to formate groups
- M06-L density functional with def2-SVP basis set for all non-metal atoms; ECP28MWB basis and associated pseudopotentials for metal atoms

Periodic Models:

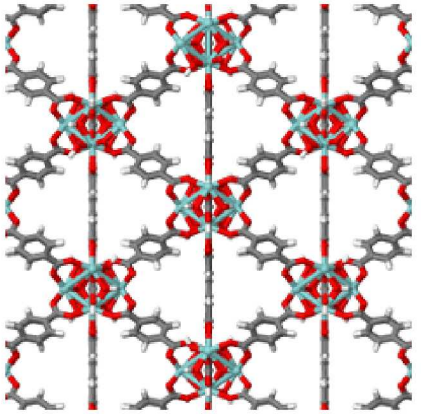

- Projector augmented wave approached implemented in VASP
- Perdew-Burke-Ernzerhof revised for solids (PBEsol) exchange correlation functional
- DFT-D3 with Becke-Jonson damping for empirical vdw interactions

$$\Delta E_{binding} = -[E_{substrate+MOF} - (E_{substrate} + E_{MOF})]$$

Positive binding energy = favorable

# Additional Binding Sites in UiO-66

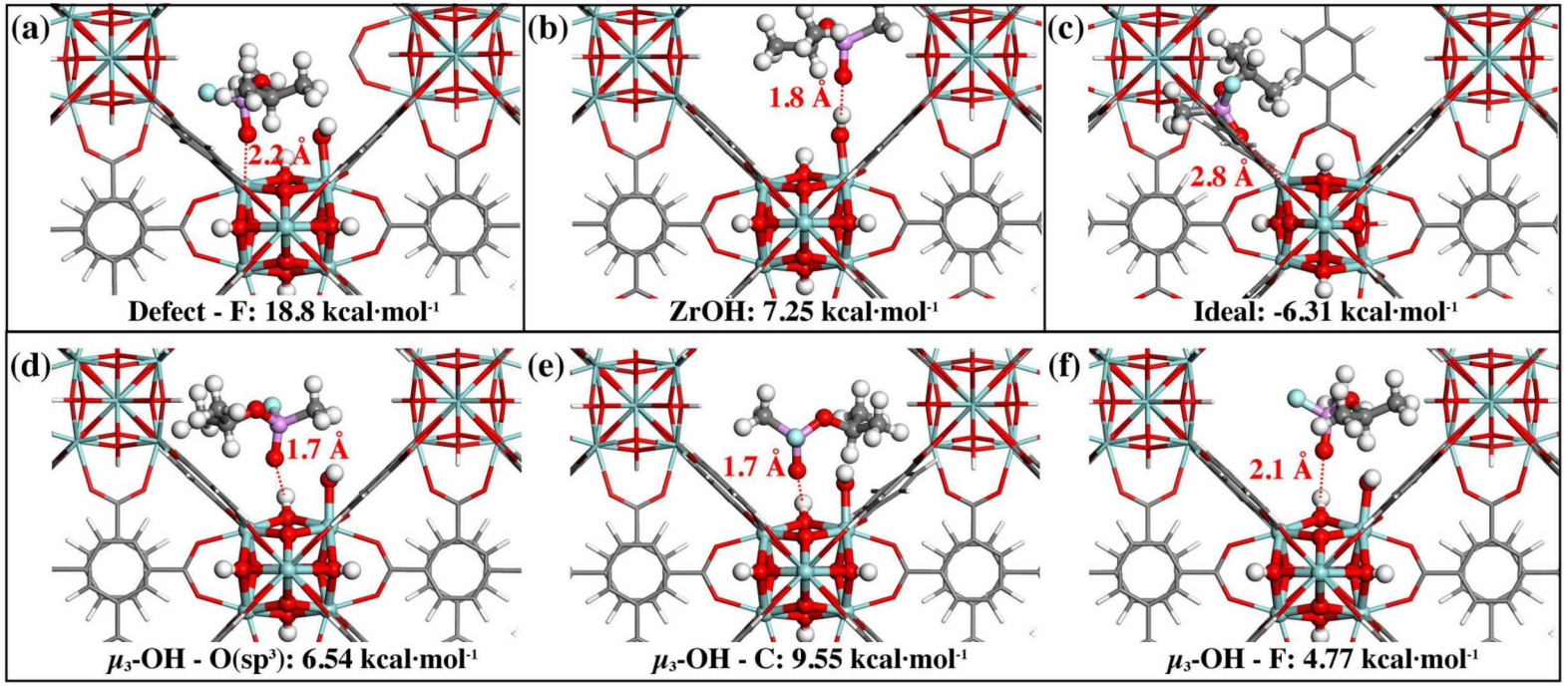


- Additional favorable binding sites for GB within UiO-66 exist; Missing linker ZrOH group, $\mu^3$-OH group
- Strong orientational effects are observed

Harvey, J.A.; Greathouse J.A.; Sava Gallis, D.F; J. Phys. Chem. C, *In Review*

# Additional Binding Sites in UiO-66

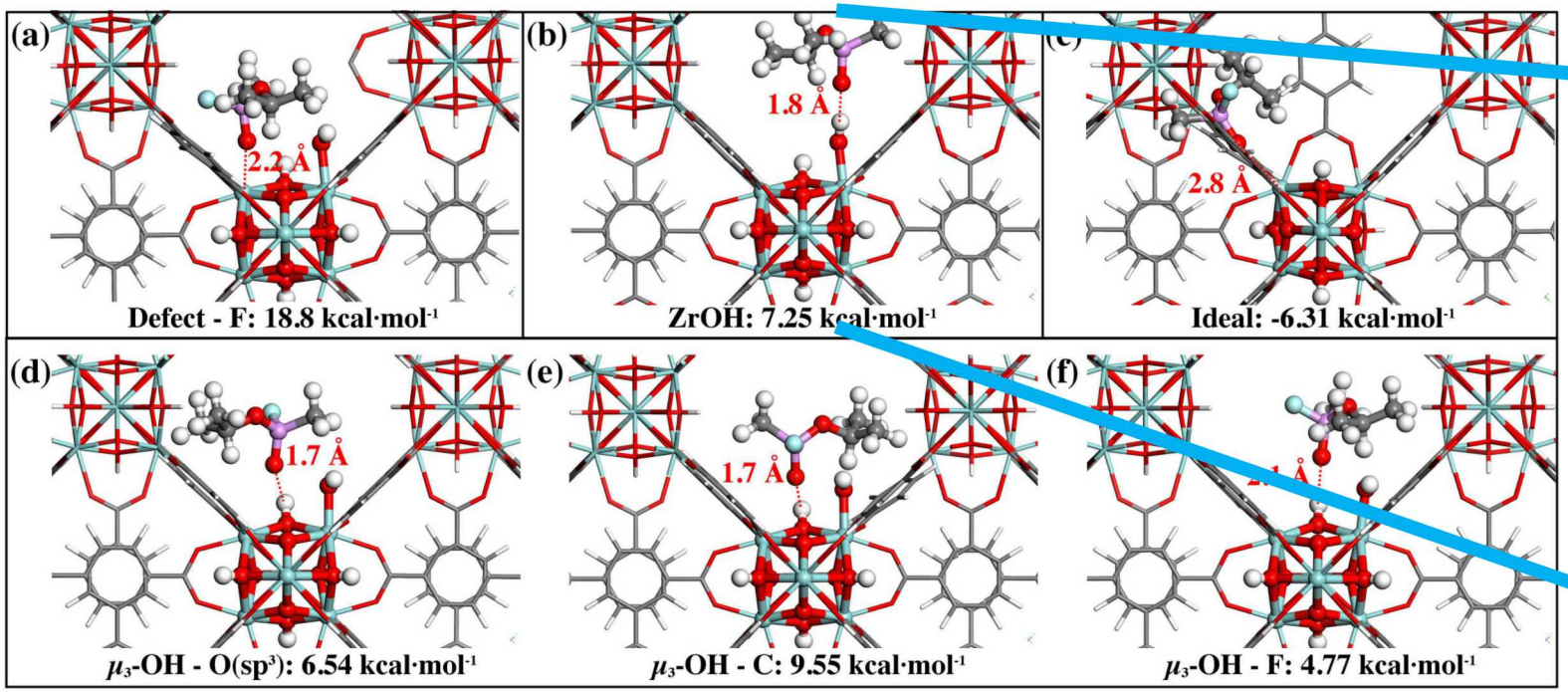


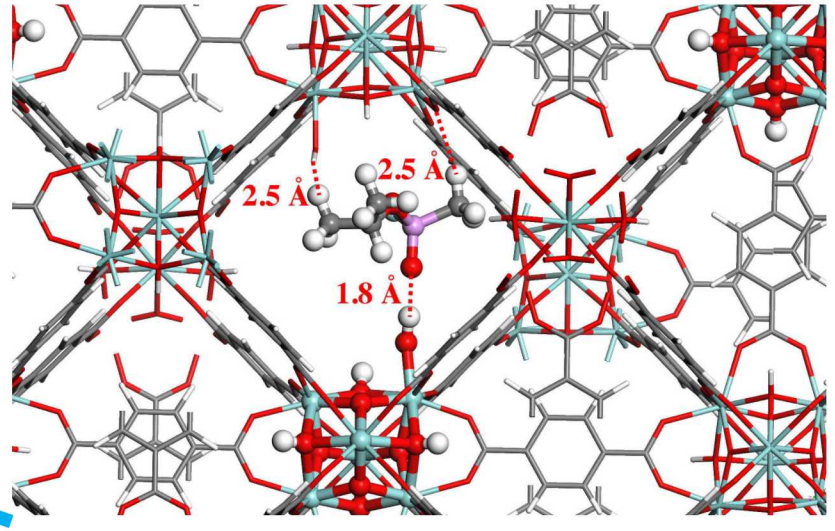


- Additional favorable binding sites for GB within UiO-66 exist; Missing linker ZrOH group, $\mu_3$-OH group
- Strong orientational effects are observed
- ZrOH binding creates interactions with entire pore → Periodic systems are necessary to capture this interaction

Harvey, J.A.; Greathouse J.A.; Sava Gallis, D.F; J. Phys. Chem. C, *In Review*

# Additional Binding Sites in UiO-66

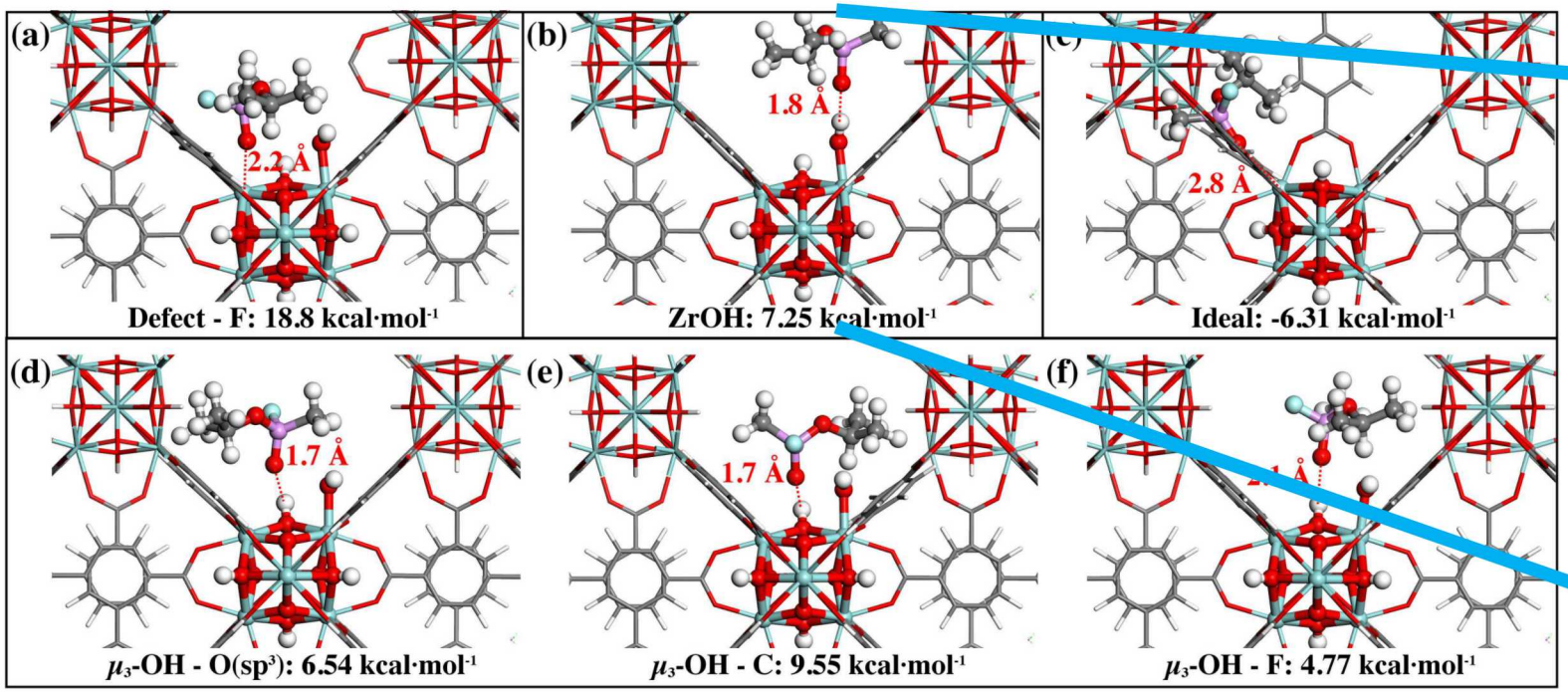


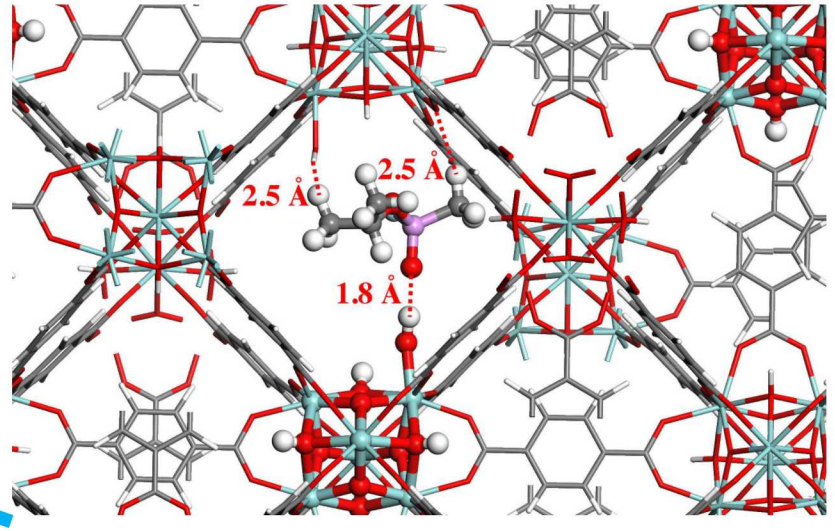


- Additional favorable binding sites for GB within UiO-66 exist; Missing linker ZrOH group, $\mu_3$-OH group
- Strong orientational effects are observed
- ZrOH binding creates interactions with entire pore → Periodic systems are necessary to capture this interaction

- Wide variety of binding sites and binding energies within UiO-66; is this observable with IR spectroscopy?

Harvey, J.A.; Greathouse J.A.; Sava Gallis, D.F; J. Phys. Chem. C, *In Review*

# Identification of Binding site via the P=O Stretch

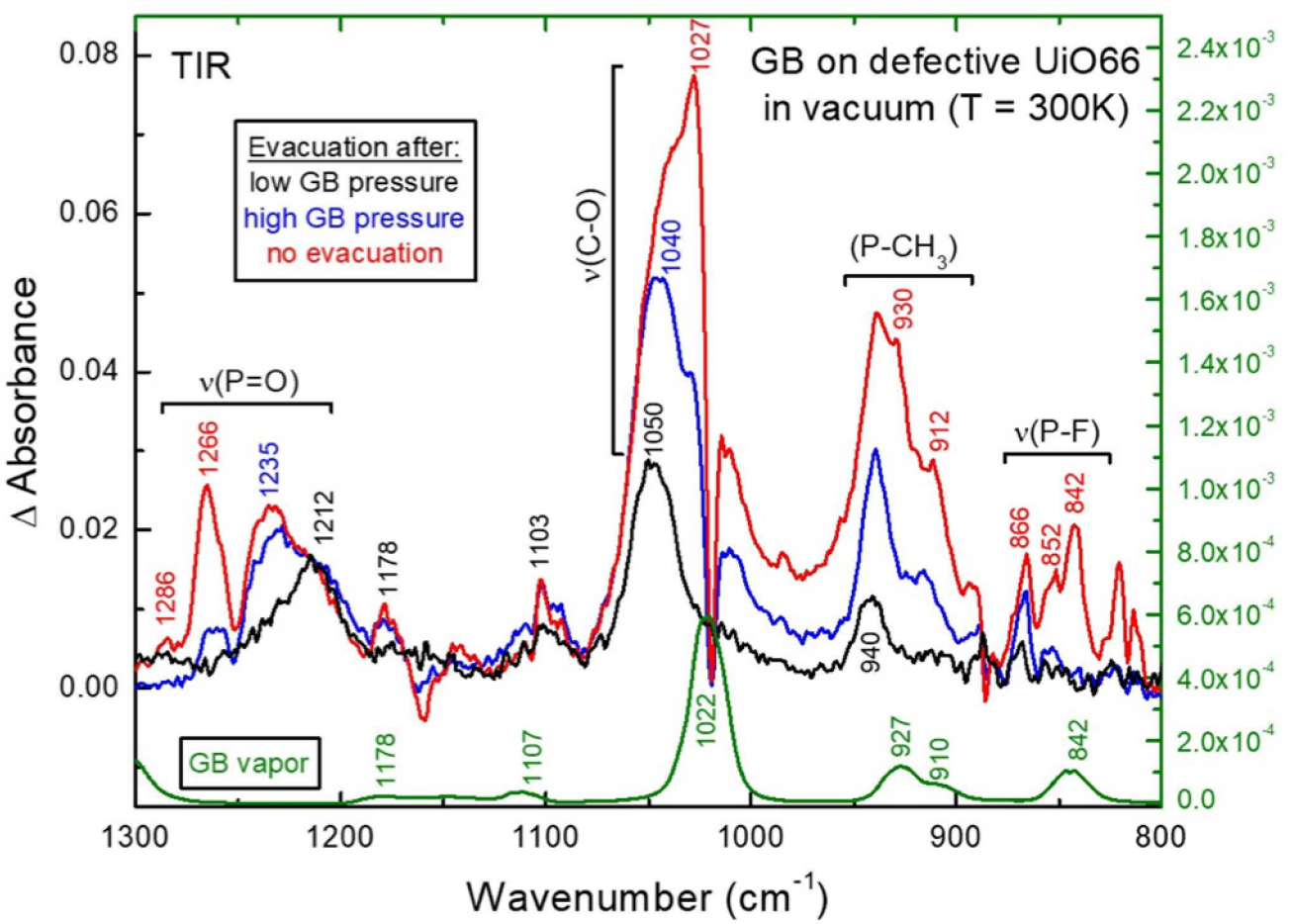


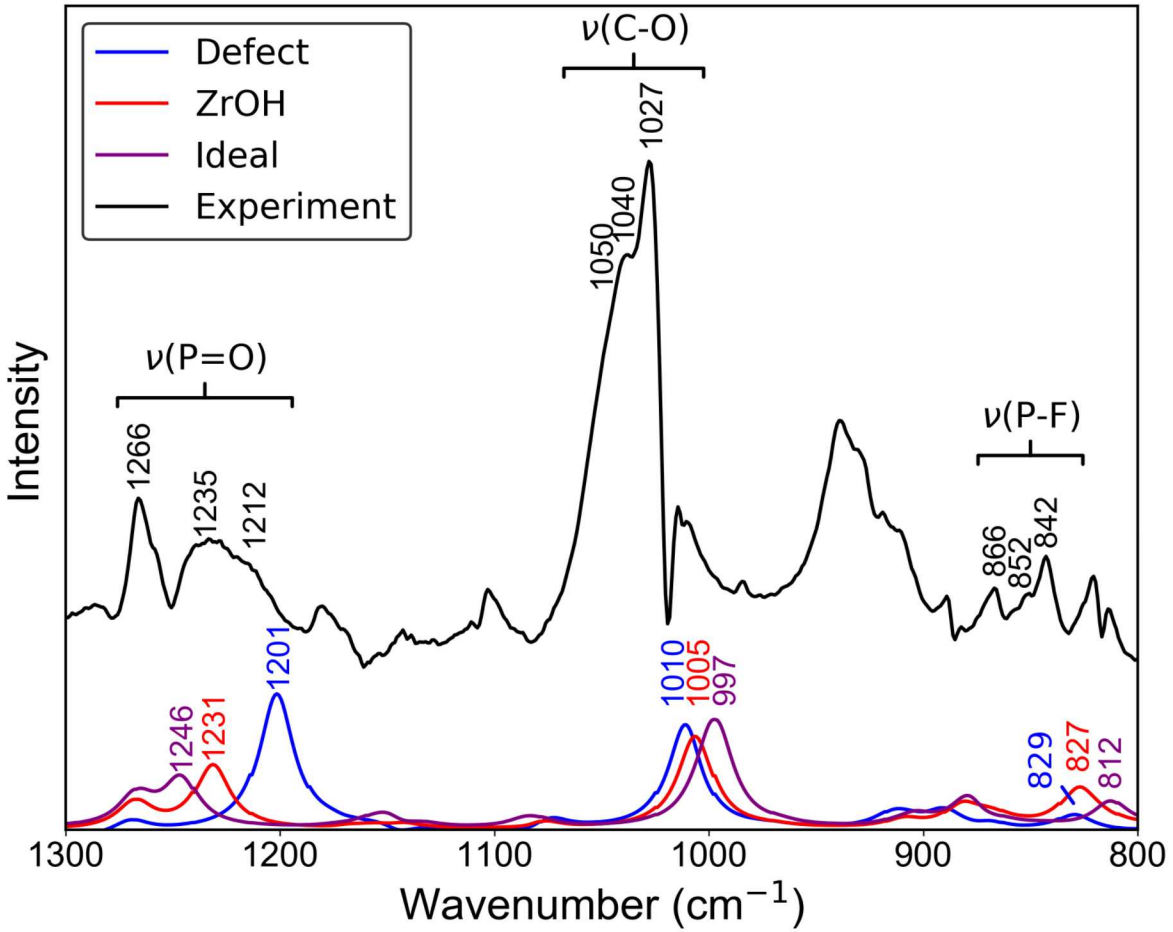


Harvey, J.A; McEntee, M.L.; Garibay, S.J.; Durke, E.M.; DeCoste, J.B.; Greathouse, J.A.; Sava Gallis, D.F; *Nat. Comm., Submitted*

# Identification of Binding site via the P=O Stretch

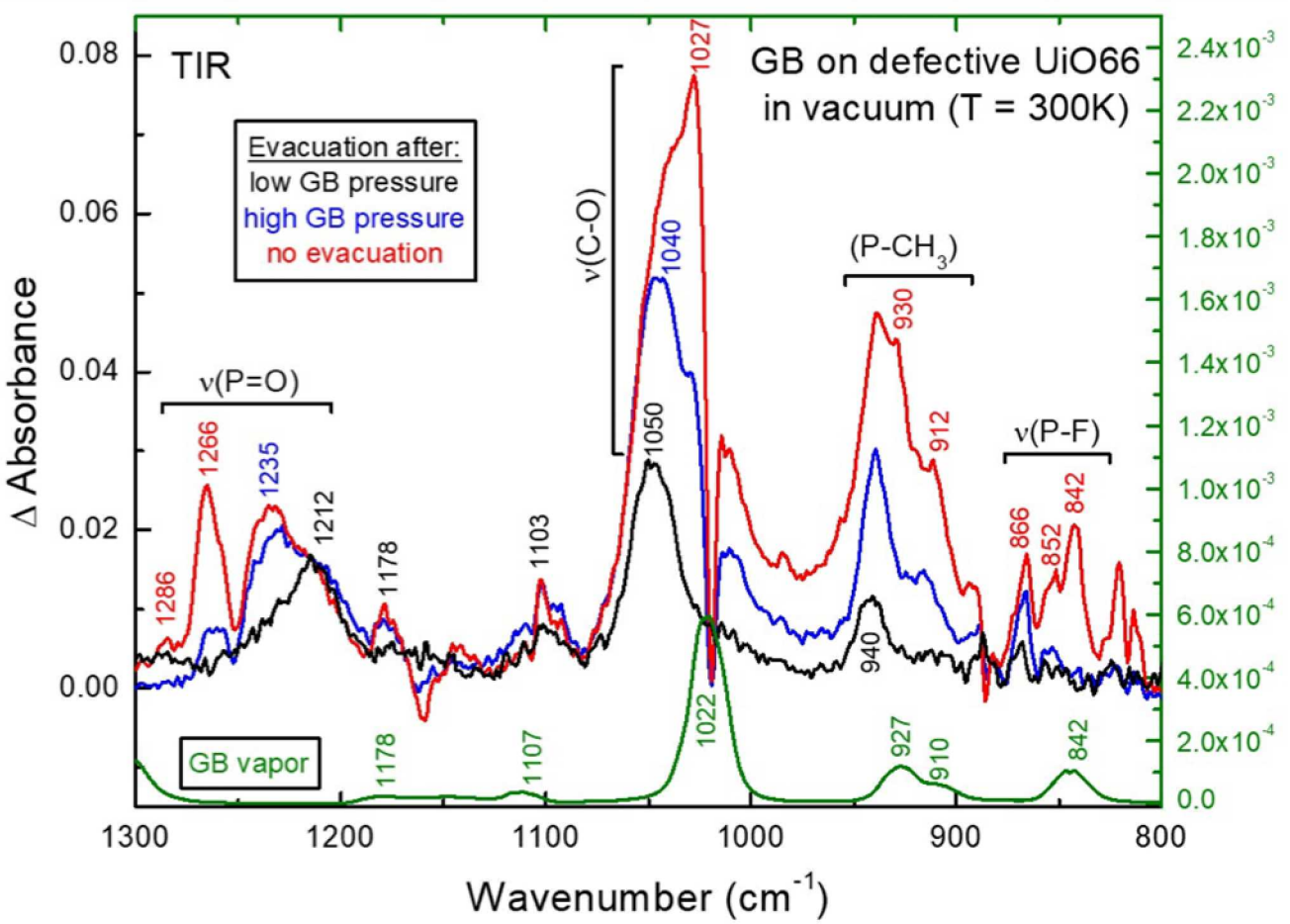


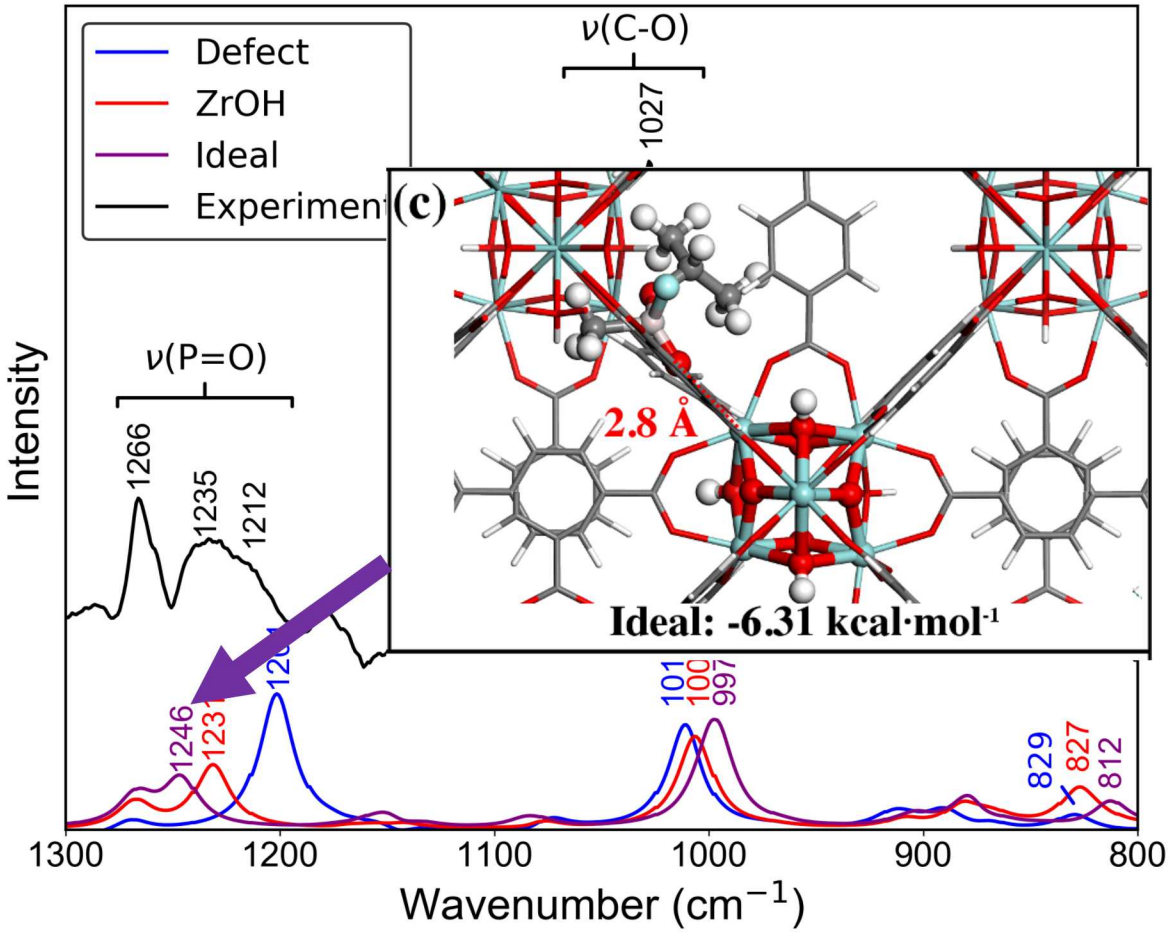


Harvey, J.A; McEntee, M.L.; Garibay, S.J.; Durke, E.M.; DeCoste, J.B.; Greathouse, J.A.; Sava Gallis, D.F; *Nat. Comm., Submitted*

# Identification of Binding site via the P=O Stretch

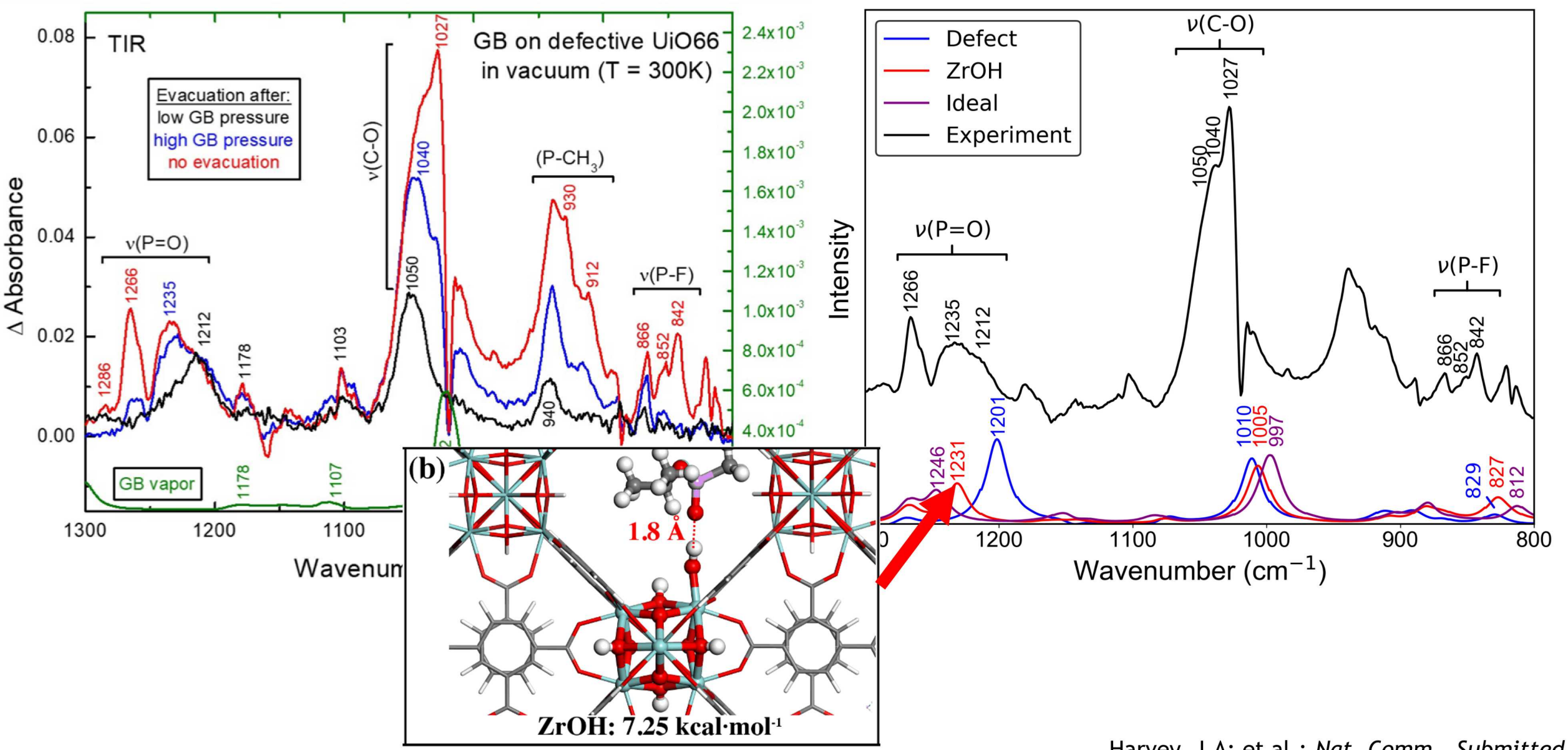


Harvey, J.A; et al.; *Nat. Comm.*, *Submitted*

# Identification of Binding site via the P=O Stretch

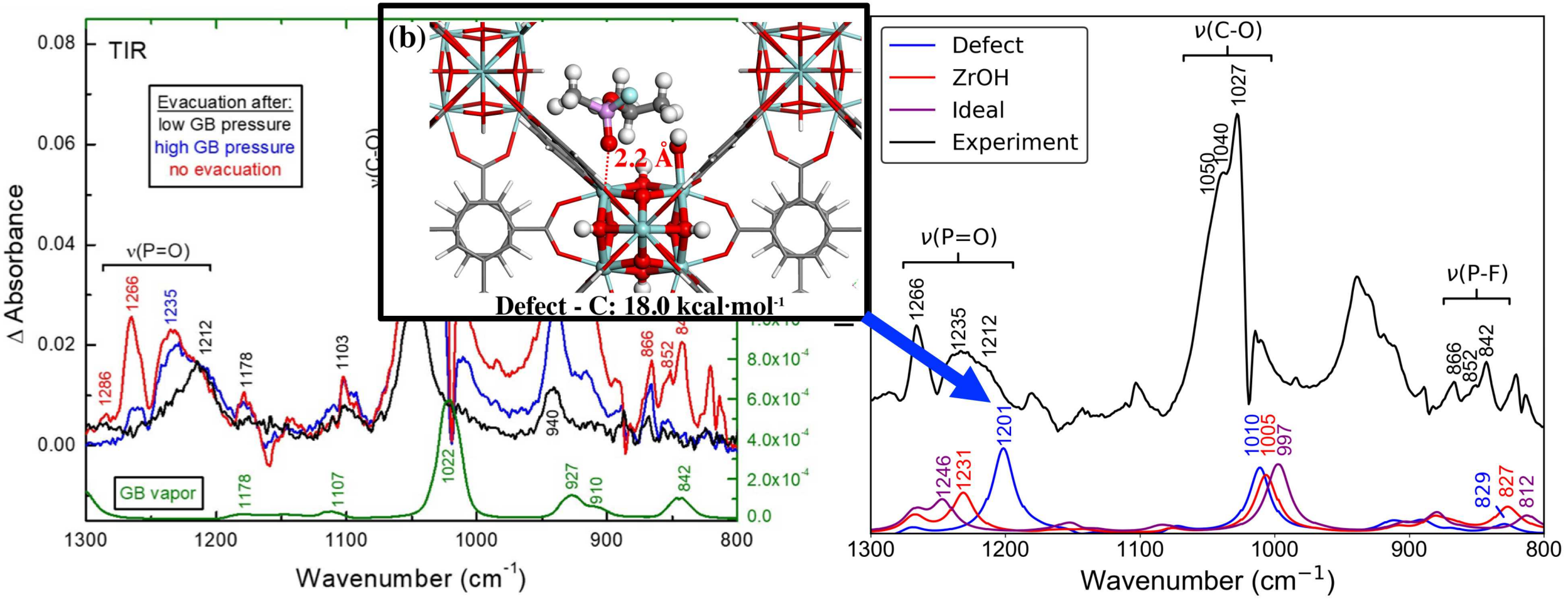


Harvey, J.A; et al.; *Nat. Comm.*, *Submitted*

# Identification of Binding site via the P=O Stretch

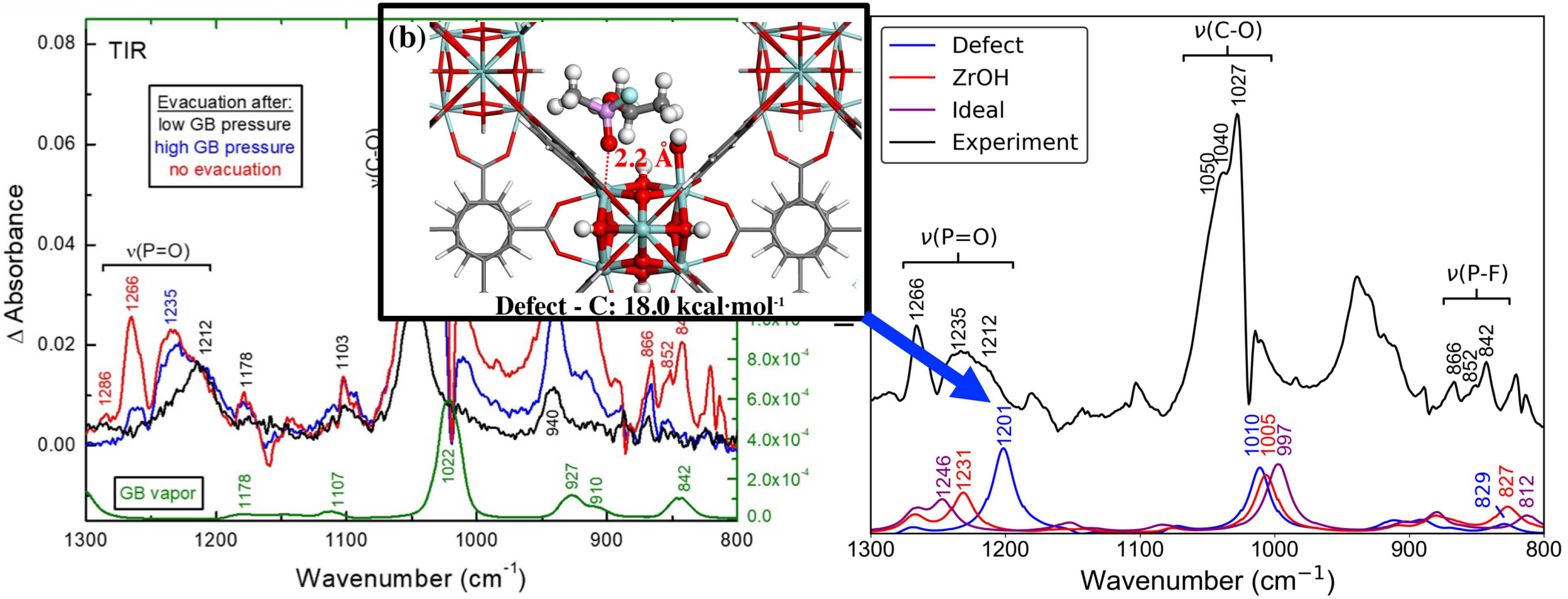


- Ideal vs defect site binding show a 50 cm-1 difference in the P=O stretch
- A 3rd site, possibly the defect created ZrOH, is observed in between the defect and ideal site binding

Harvey, J.A; et al.; *Nat. Comm., Submitted*

# Exploration of ZrOH site binding

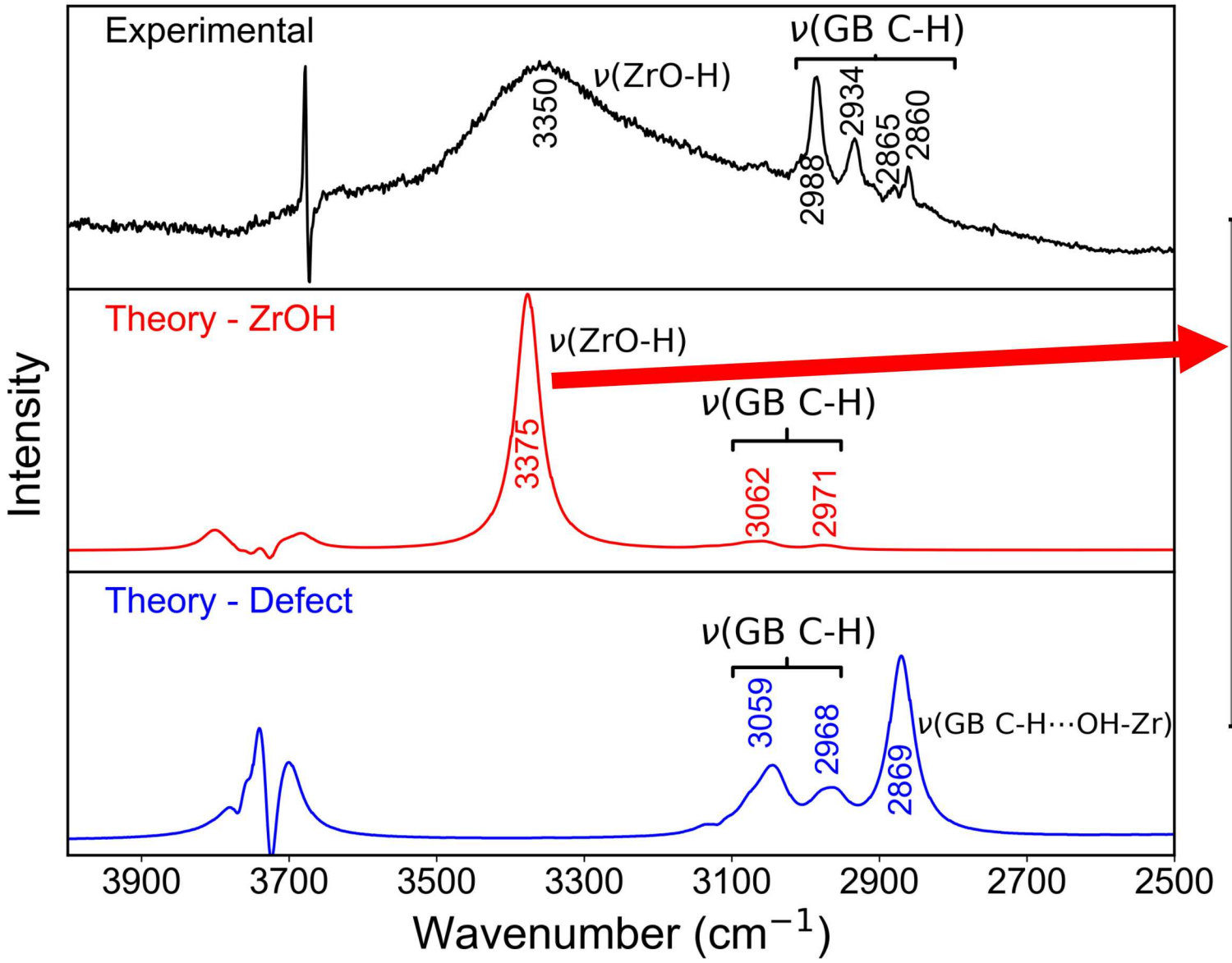


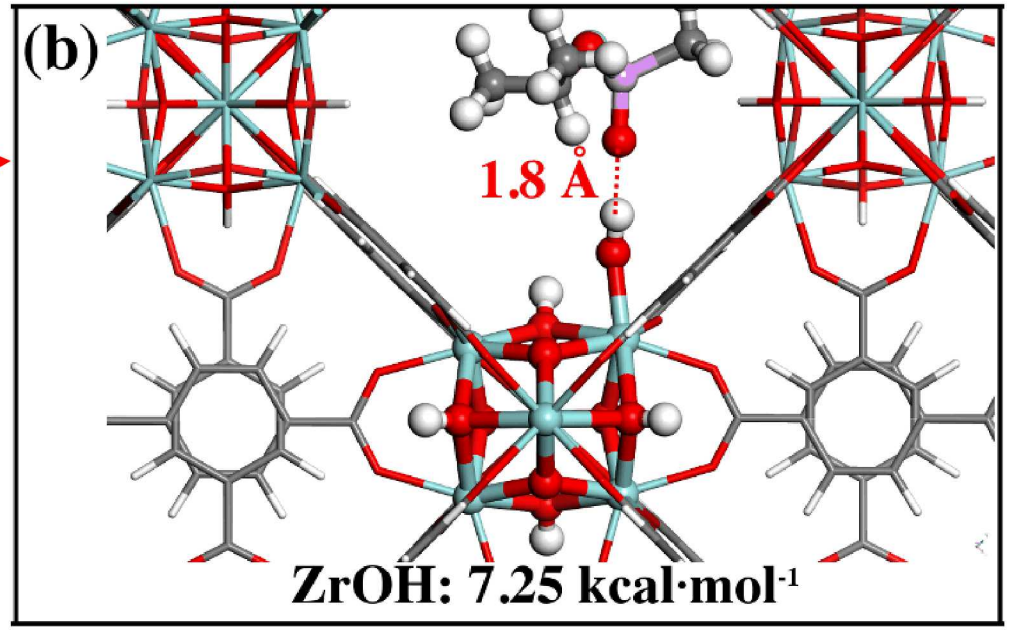


Harvey, J.A; et al.; *Nat. Comm.*, *Submitted*

# Observation of Orientation at Binding Site

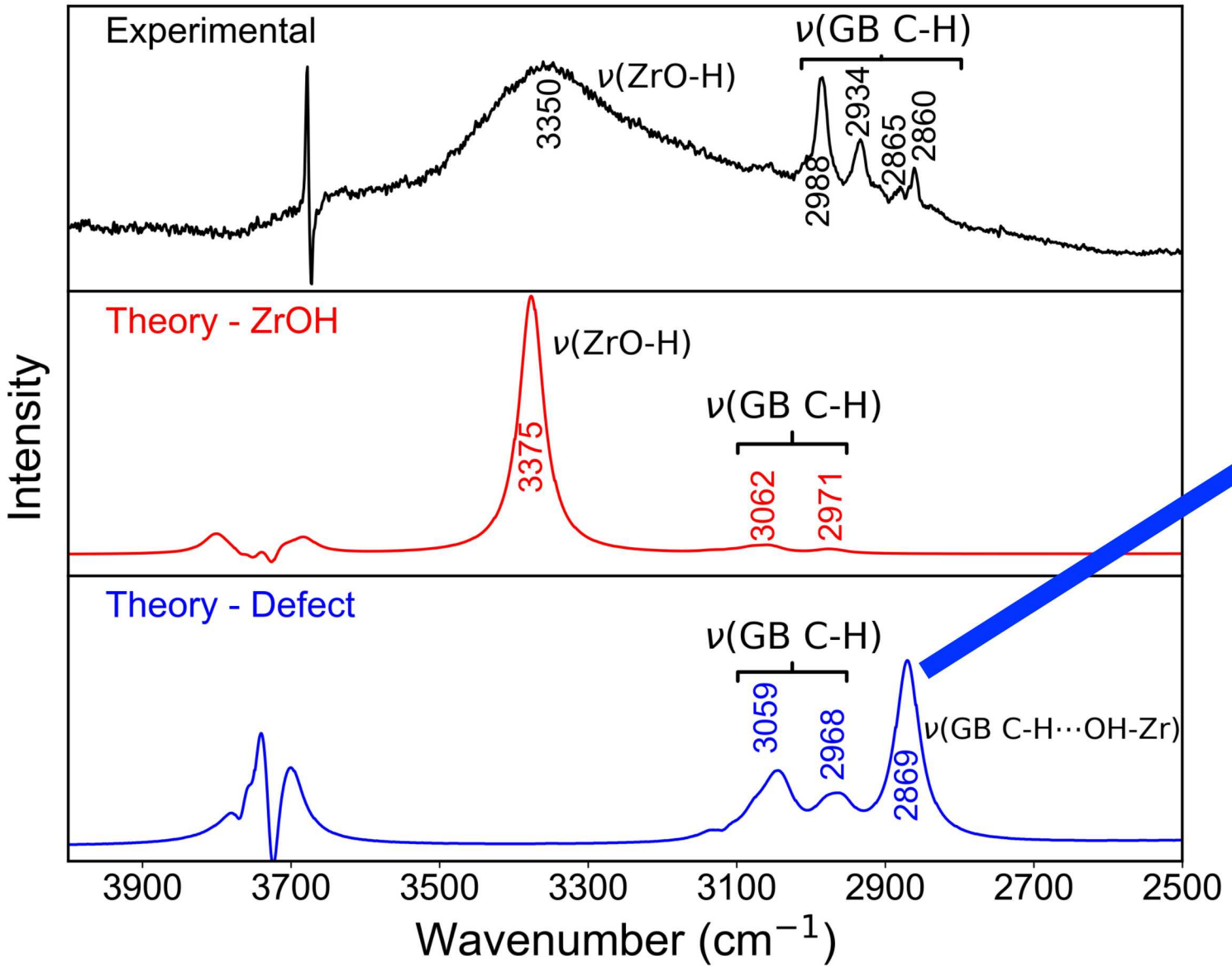


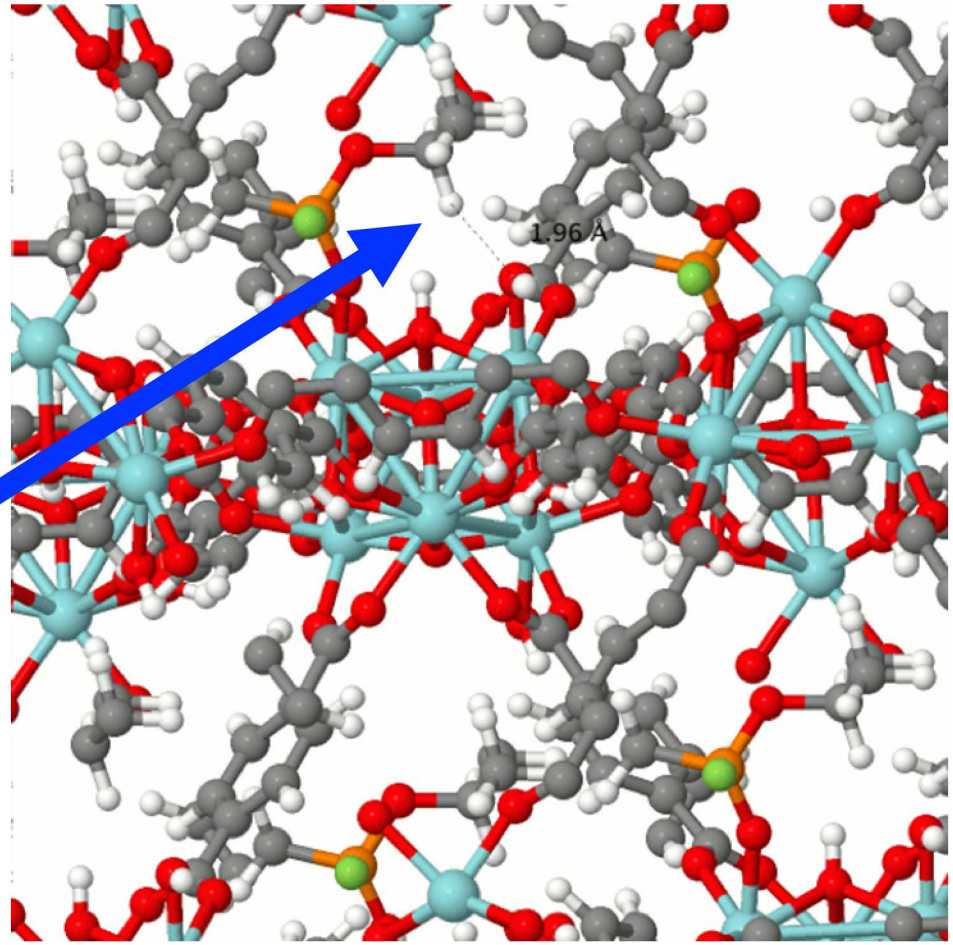


Harvey, J.A; et al.; *Nat. Comm., Submitted*

# Observation of Orientation at Binding Site

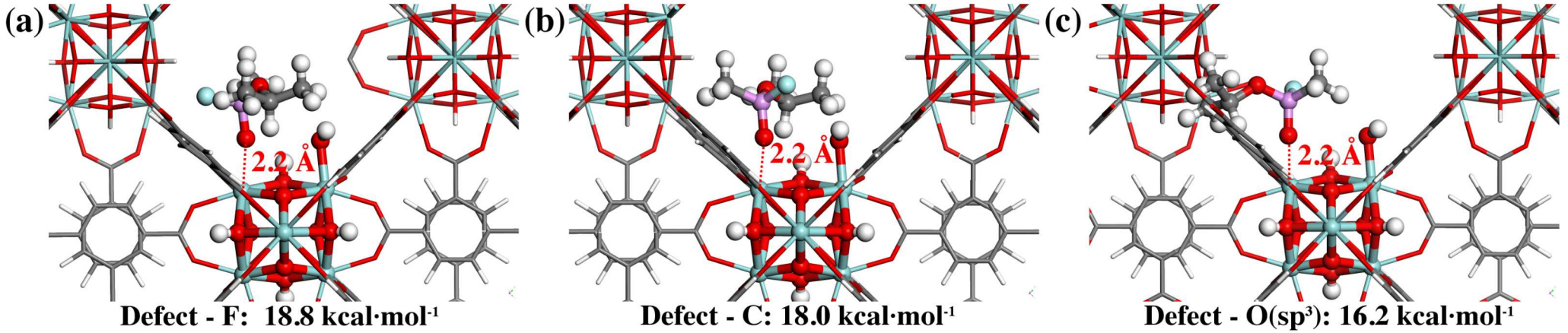


Defect - F: 18.8 kcal·mol$^{-1}$ Defect - C: 18.0 kcal·mol$^{-1}$ Defect - O(sp$^3$): 16.2 kcal·mol$^{-1}$

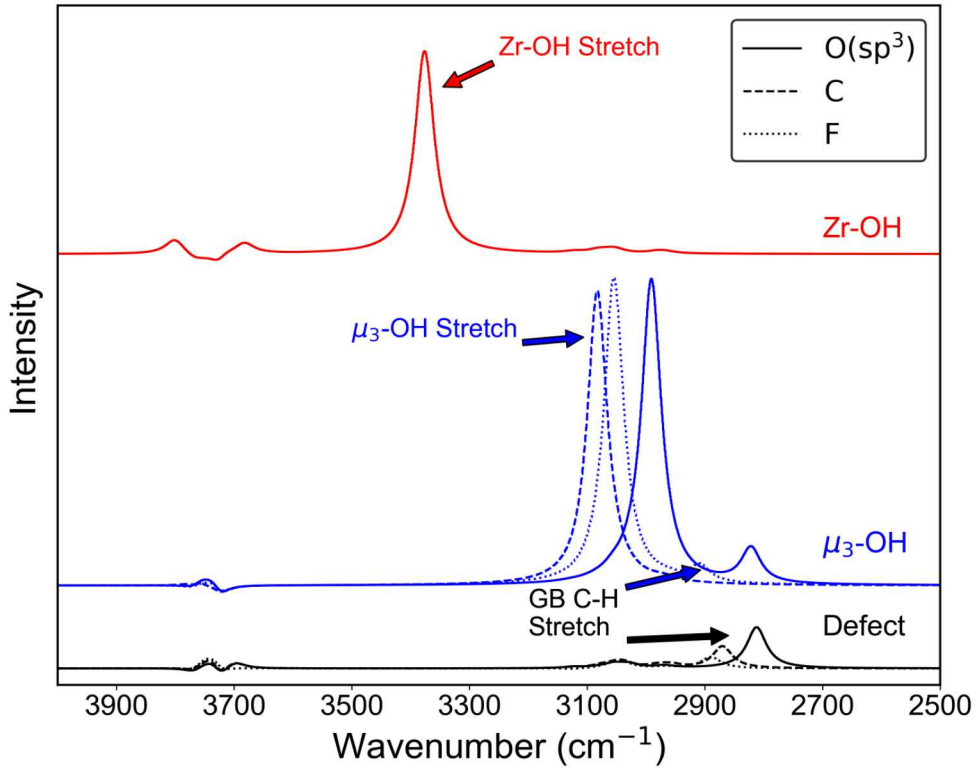


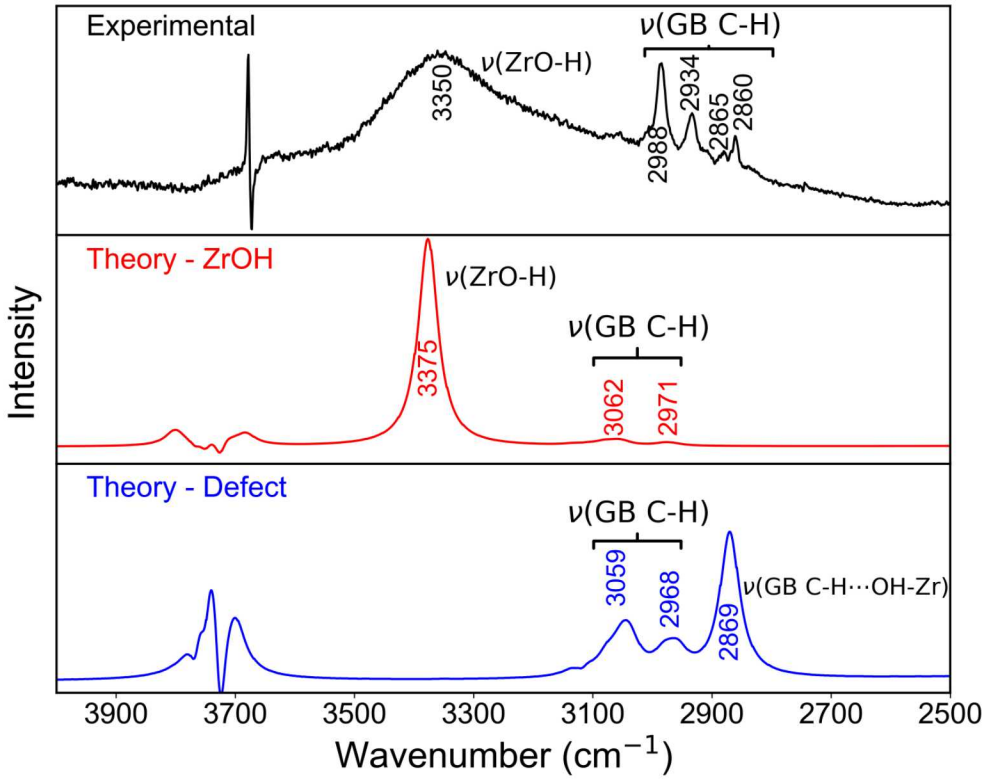

# Possibility of $\mu_3$-OH binding

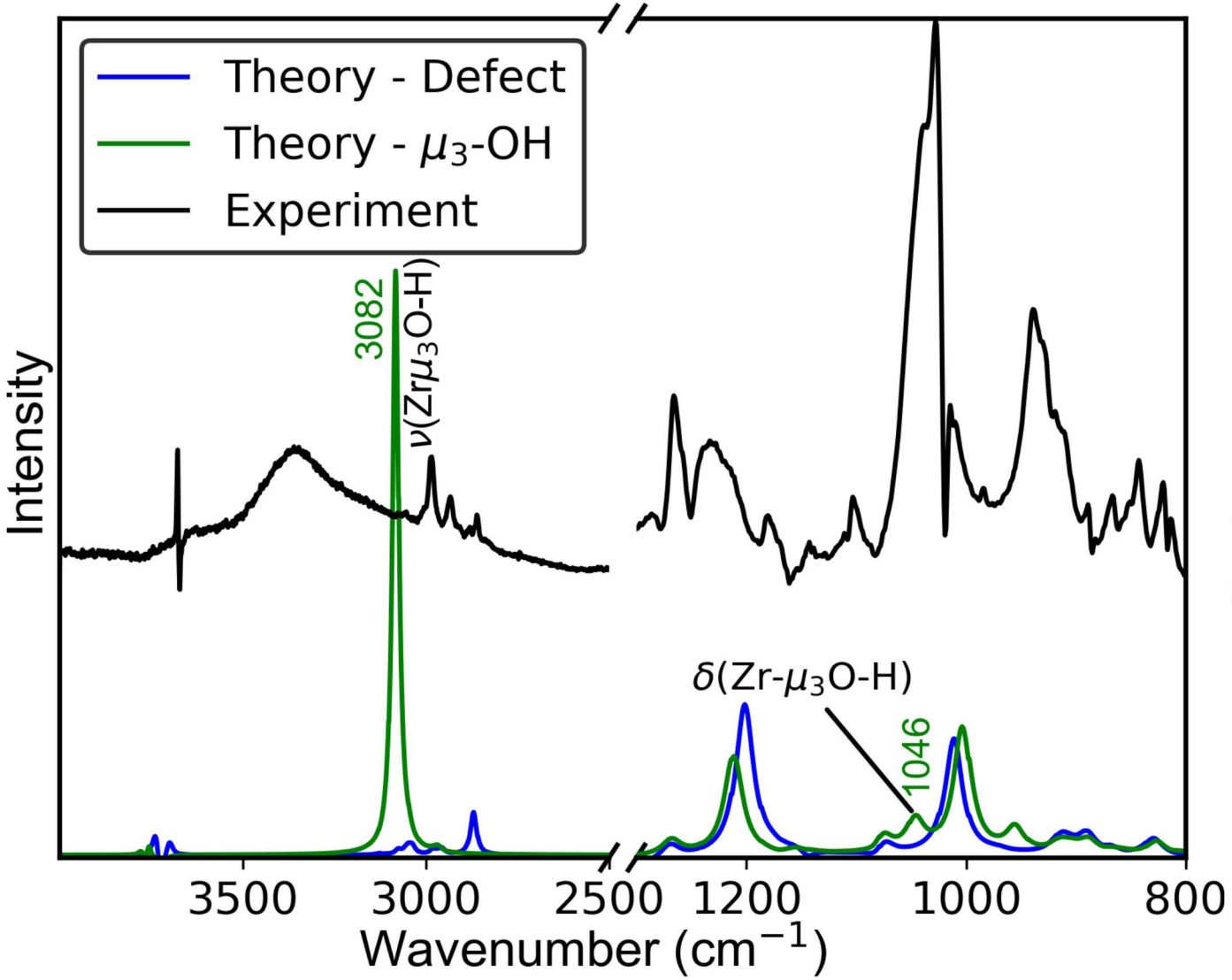


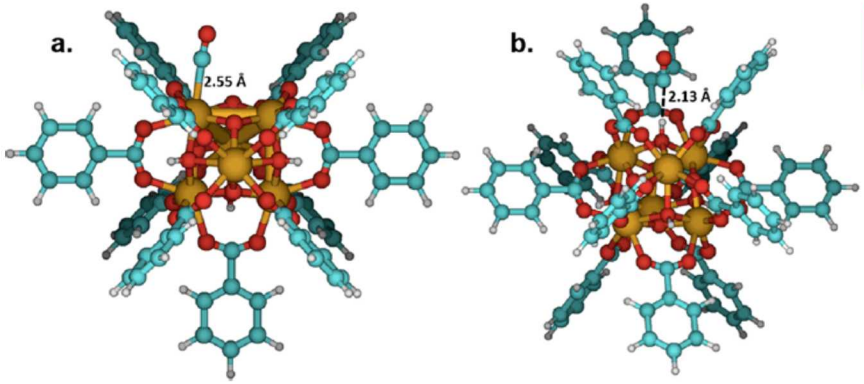


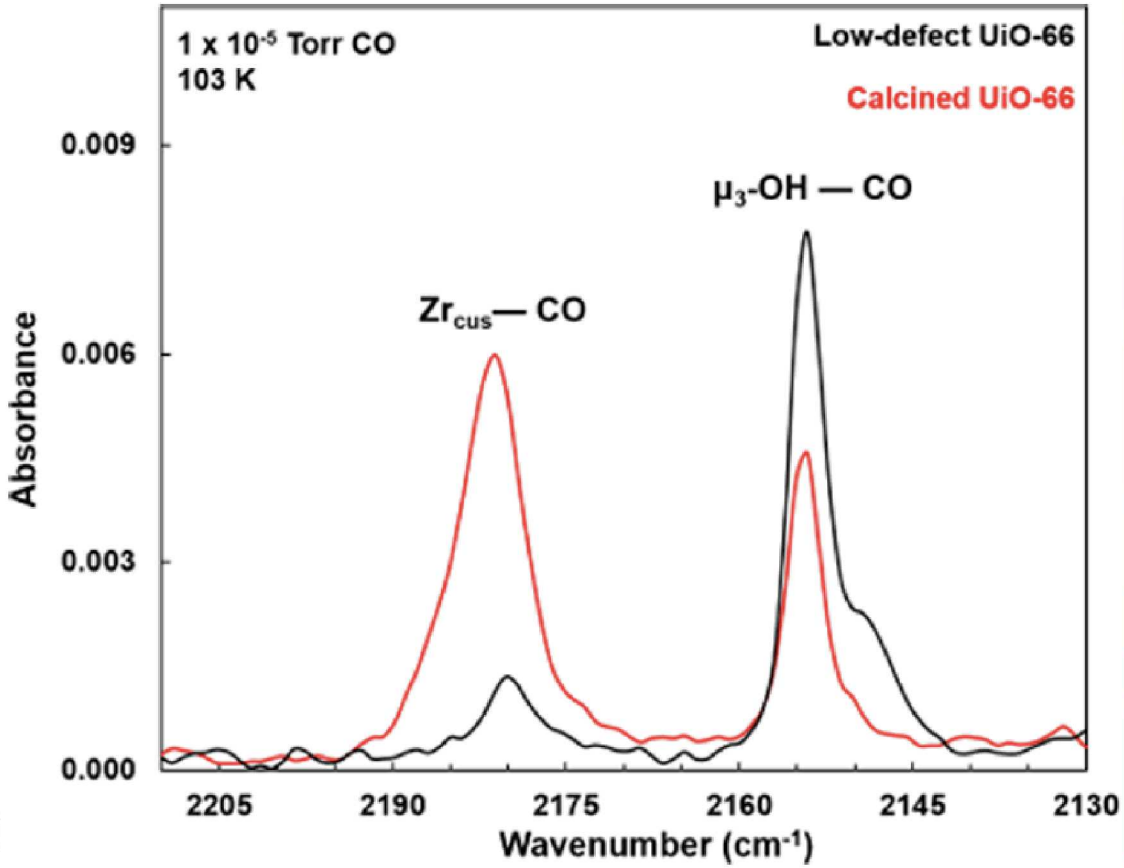

# Possibility of $\mu_3$-OH binding

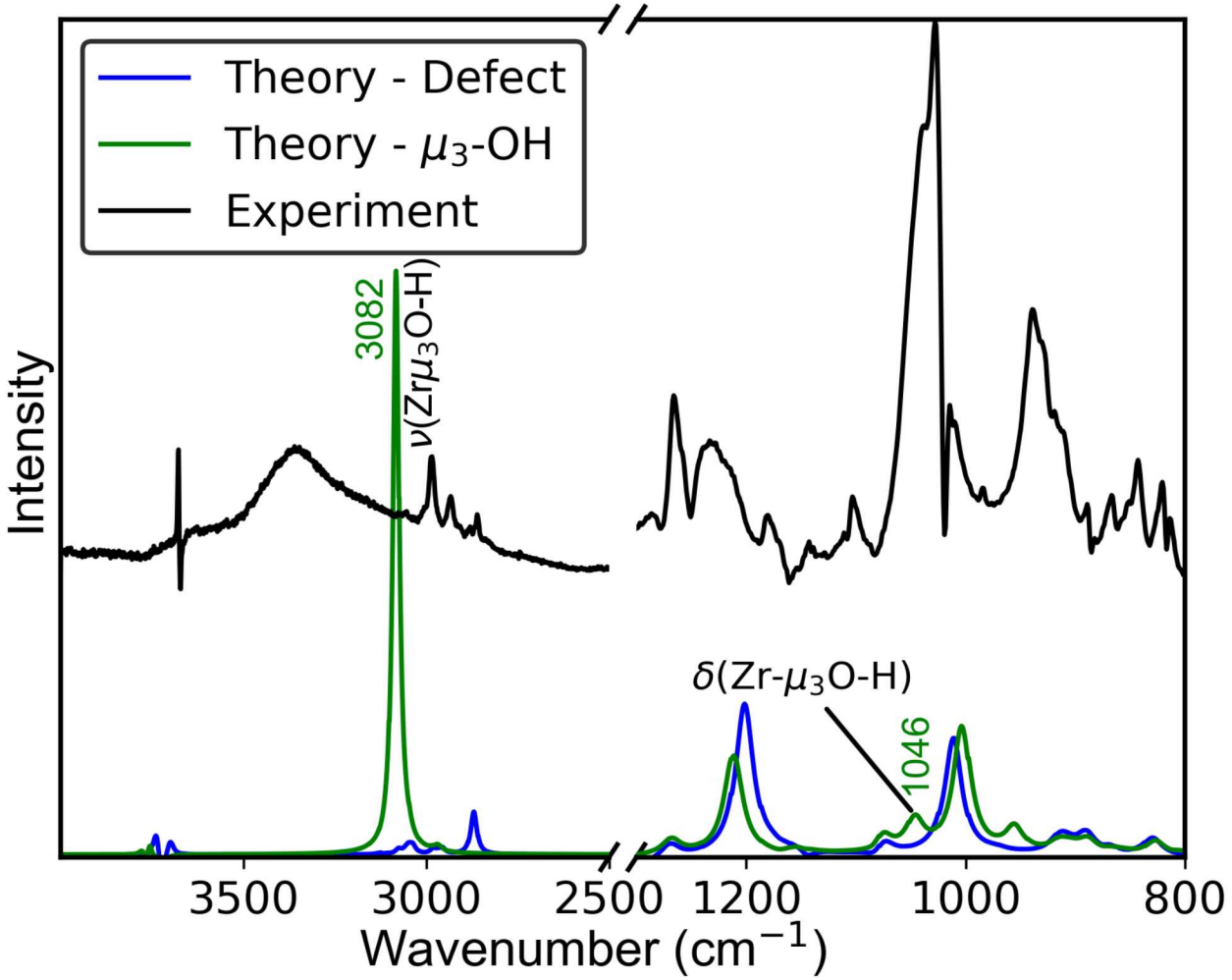


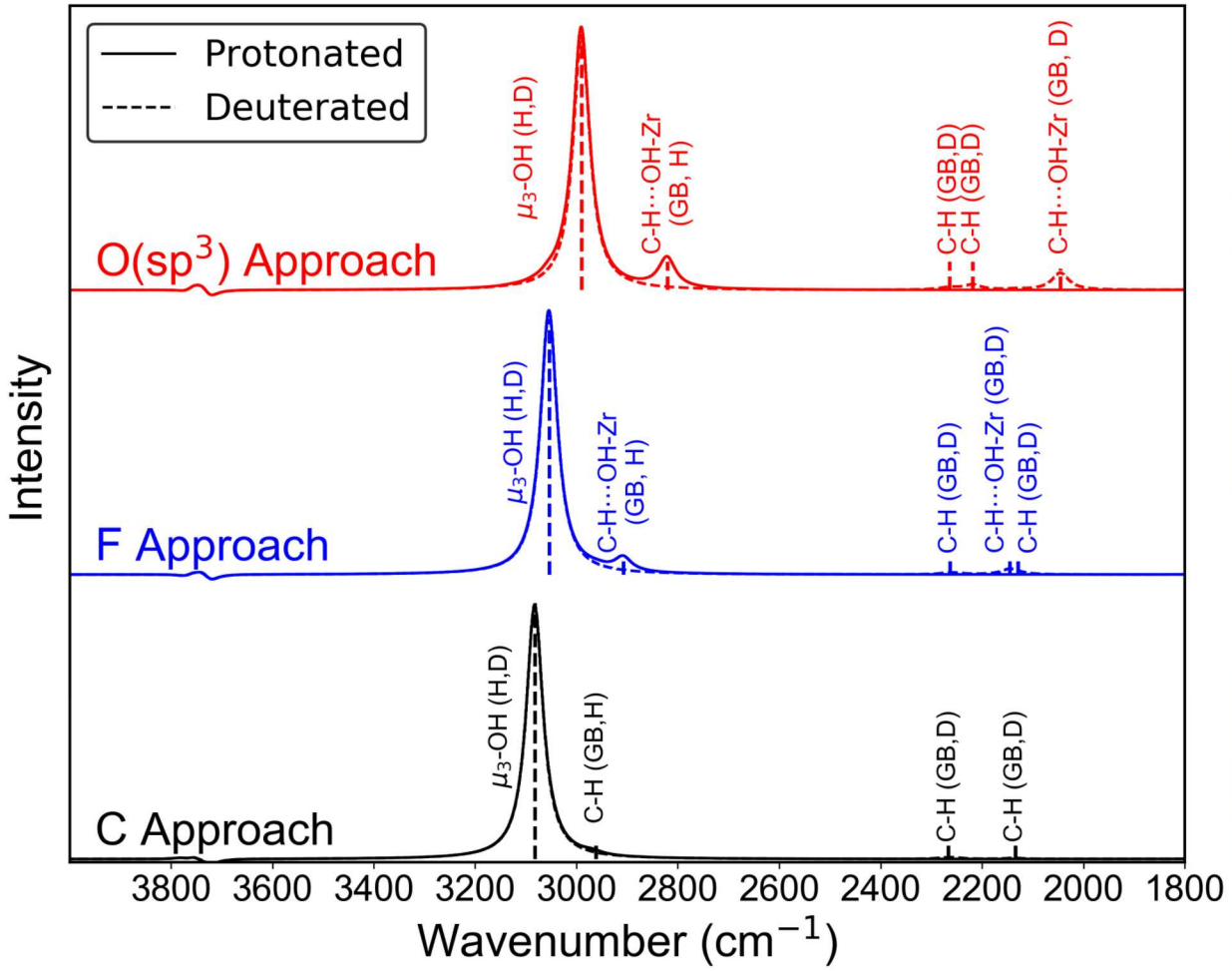

# Gas Phase Degradation in UiO-66

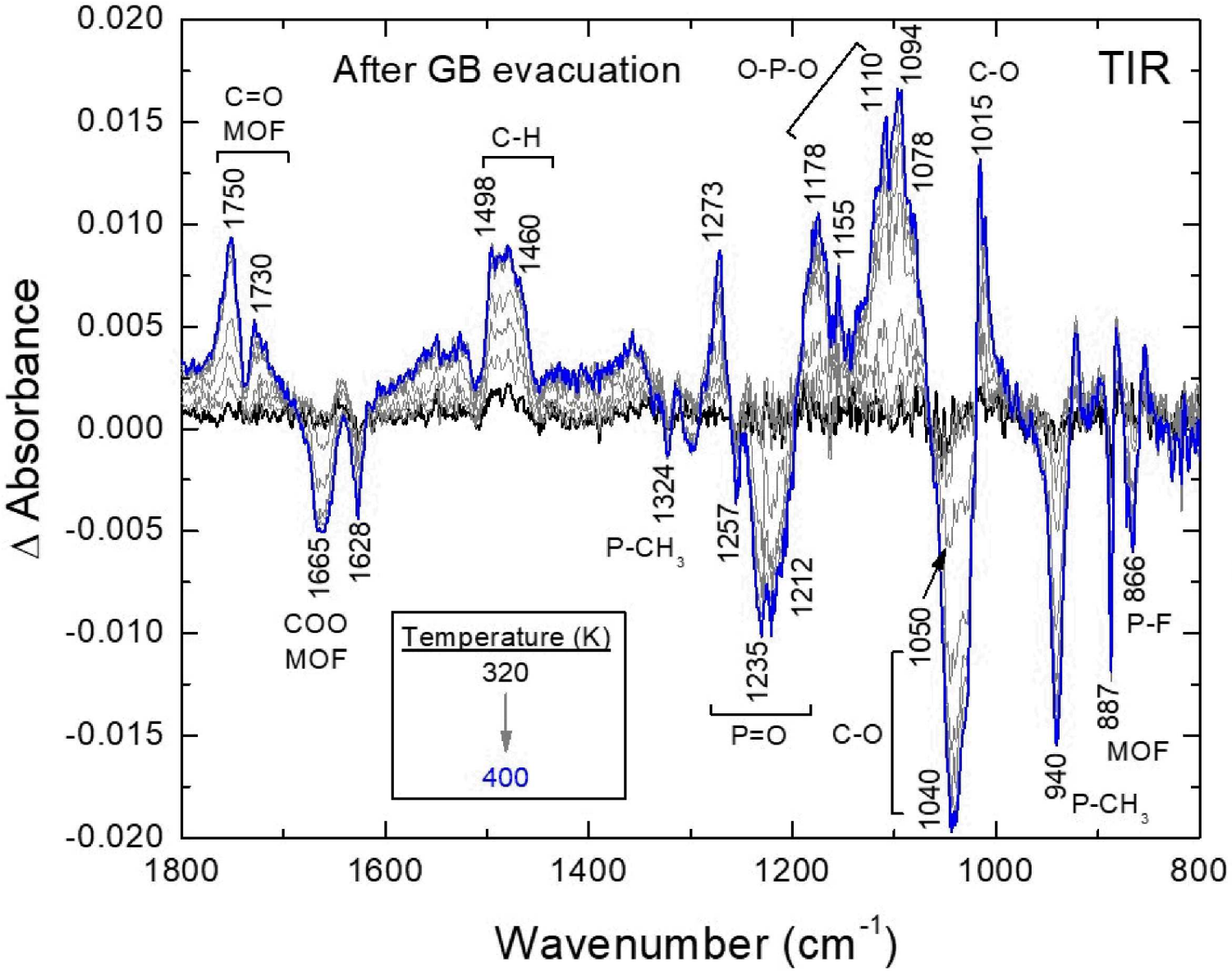


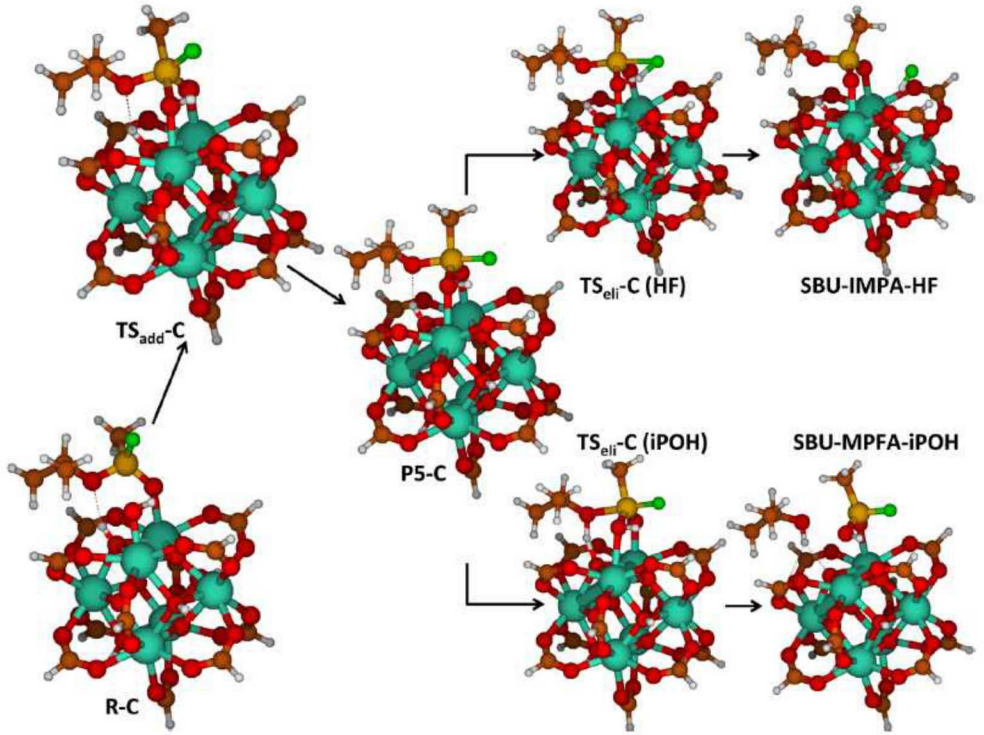

# Gas Phase Degradation in UiO-66

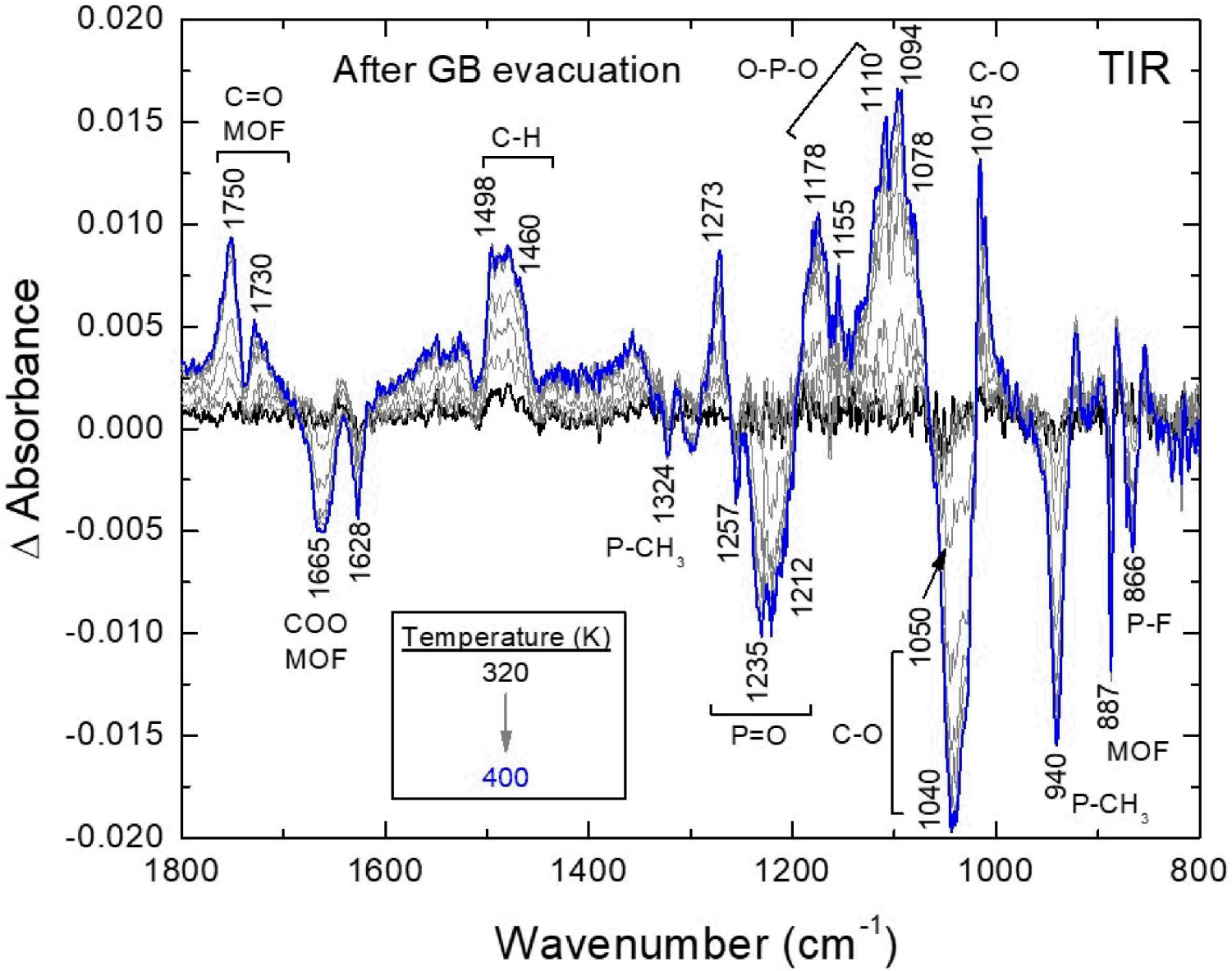


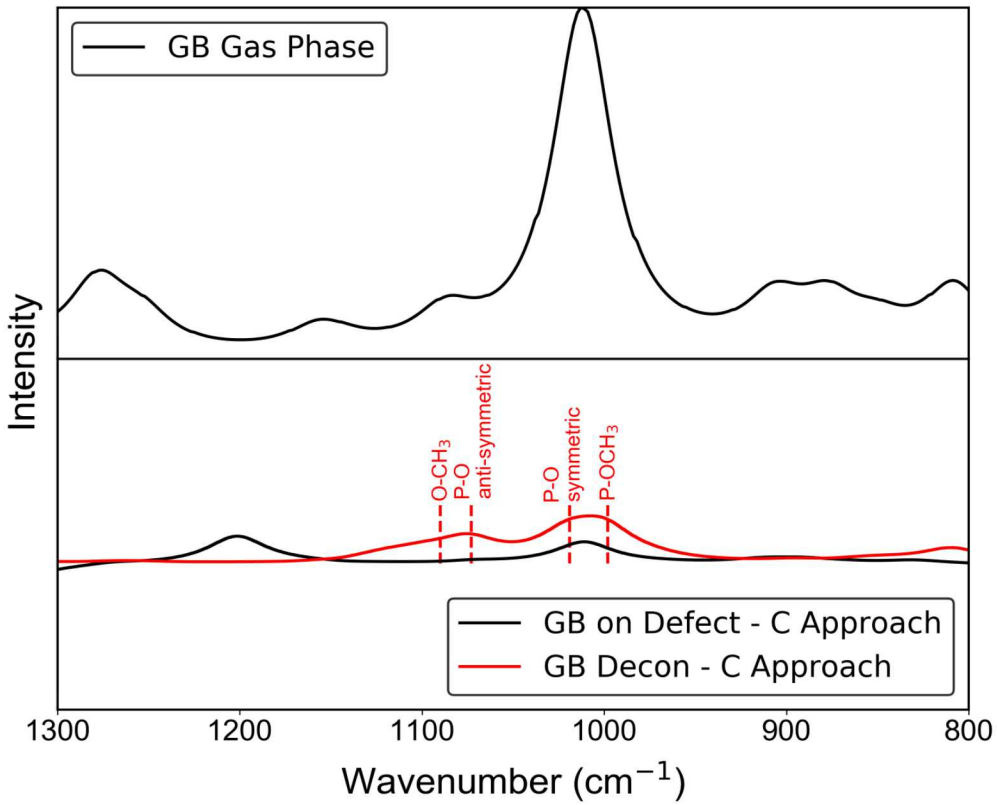

# Conclusions

## Metal, linker, and cluster model play distinct role in binding energy

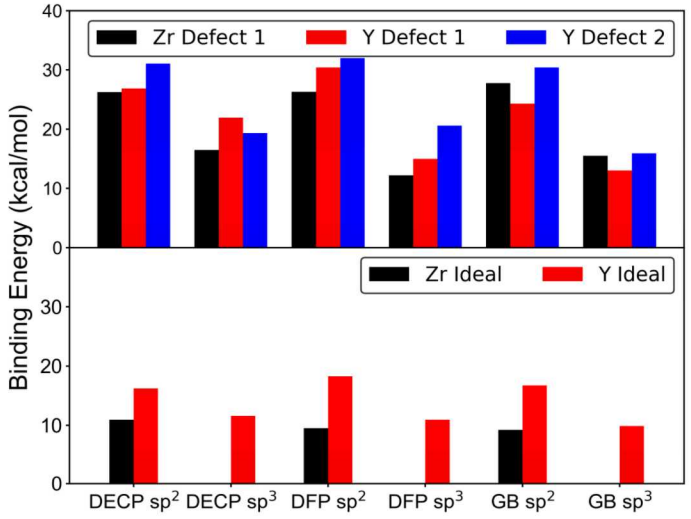


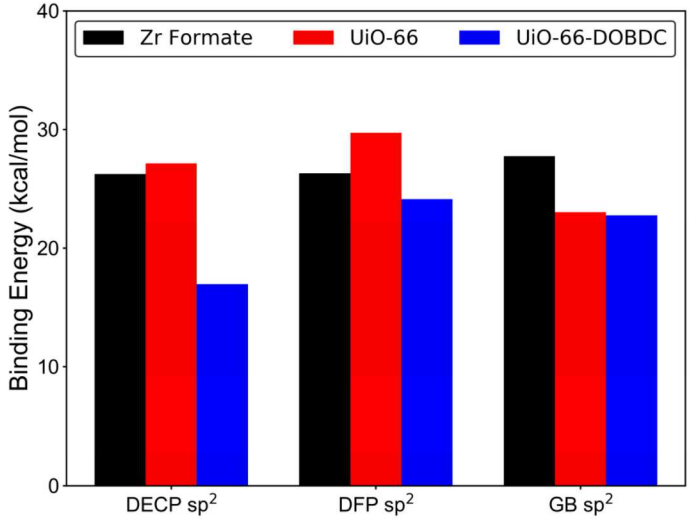


## Binding sites are directly observable via IR spectroscopy

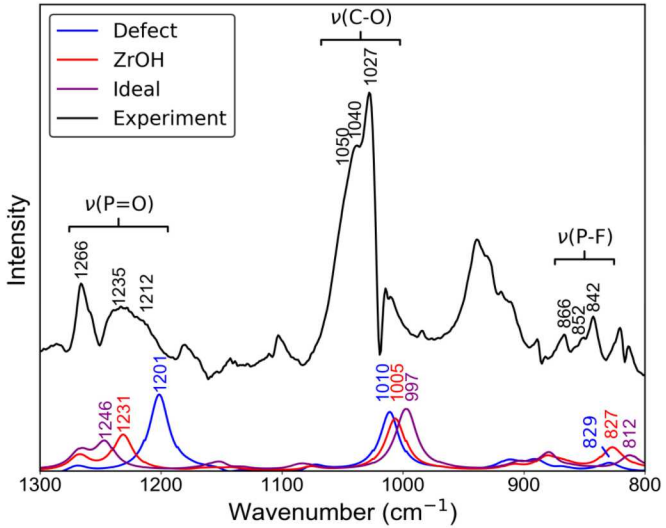


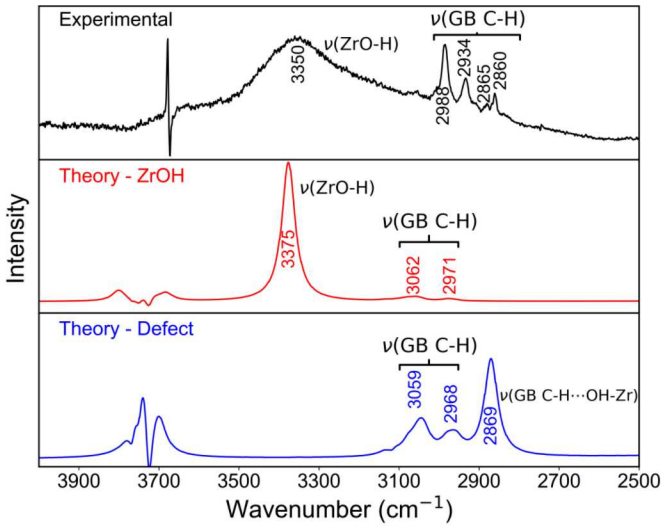


## Gas phase degradation of GB in UiO-66